3
Characterization and Control of Physical Quality Factors During Freeze-Drying of Pharmaceuticals in Vials

Julien Andrieu and Séverine Vessot

3.1
Introduction

While a majority of pharmaceutical drugs are stable enough to be preserved in cold chambers at 4 °C before their use, some types of these labile products, and especially those including living viruses (proteins or vaccines), have to be dehydrated by very mild drying methods at very low temperature to be preserved a few months in the solid state, inserted in porous dehydrated solid matrices, before their utilization after rehydration. Mostly manufactured in the developed countries of the north hemisphere, these thermosensible pharmaceutical products can then be stored and shipped all around the world in ambient conditions without any cold chain as is the case with liquid solutions. Consequently, freeze-drying processes which take place at very low temperature relative to convective (tunnel or oven) drying or to spray-drying, are less damaging separation processes for labile biological and pharmaceutical products. Nevertheless, loss of therapeutic activity or low storage stability can be observed.

Figure 3.1 presents a global scheme of the principal basic phenomena occurring during a conventional freeze-drying process.

The productivity of these processes is very low and the operating costs are very high due to the necessity of operating under high vacuum and at very low temperatures. These constraints lead to very low drying rates and, hence, to very long drying times. For example, in the pharmaceutical industry, usual drying times for commercial protein formulations in glass vials at standard sublimation conditions, sublimation temperature $T = -25$ °C, total pressure $P = 20$–30 Pa, are around 24–48 h. However, freeze-drying is more often the only separation process that can be used to stabilize therapeutic proteins or vaccine formulations. Freeze-drying preserves most of their therapeutic activity even if some degradation inevitably occurs during the dehydration process itself or during the following storage period.

Typically, the aqueous protein solution is filled into glass vials and then these vials are loaded onto temperature-controlled shelves in the product chamber of the freeze-dryer, the temperature of which is rapidly lowered in order to freeze the solution quite

Modern Drying Technology Volume 3: Product Quality and Formulation, First Edition.
Edited by Evangelos Tsotsas and Arun S. Mujumdar.

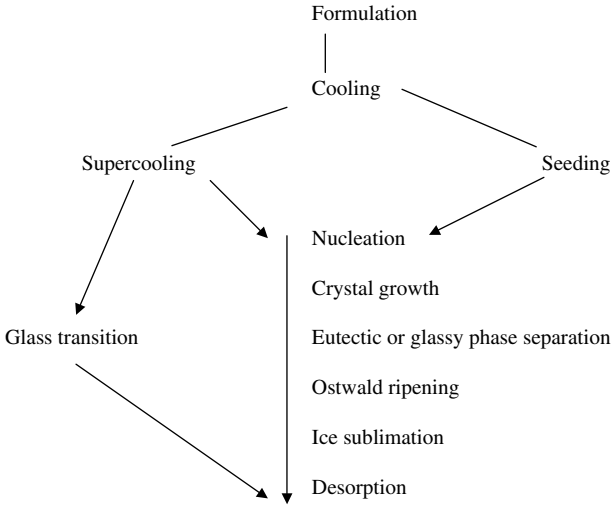

Fig. 3.1 Scheme of the different steps of a freeze-drying process.

rapidly. Next, the vacuum is applied on the two chambers (product and condenser) and the temperature of the cryofluid circulating through the shelves is increased to supply, successively, the ice sublimation enthalpy and the desorption heat of the residual unfrozen water. Thus, the optimization of pharmaceutical protein freeze-drying cycles consists mainly in adjusting the formulation parameters, the freezing rate and the primary and secondary drying operating conditions (shelf temperature, total gas pressure) to reach rigorous imposed standards of therapeutic activity and stability criteria.

3.2 Characterization Methods of the Key Quality Factors During Freeze-Drying of Pharmaceuticals in Vials

Quality achievement requires that cooling rates, temperature levels, final mean moisture contents and water gradients through the dried-out cake should be carefully controlled all along the freeze-drying process. Uncontrolled temperature levels can induce undesirable color changes and, principally, material collapse with a loss of mechanical resistance and therapeutic activity.

Moreover, excessive moisture gradients in the freeze-dried matrix can result in significant material shrinkage leading to the build-up of stresses and possible crack formation inside the dried-out bulk cake. This risk of crack formation is critical during the setting-up and the optimization of drying cycles in different industries: ceramics, food (rice, pasta), wood, and so on. Similarly, the quality factors or the end-use properties of therapeutic proteins or vaccines freeze-dried in vials (morphological, mechanical, color, therapeutic activity, stability, etc.) are strongly related to the

formulation parameters and the operating conditions of freezing and drying steps. Consequently, a fundamental scientific approach to this problem, namely, how to avoid or to reduce the collapse and the crack formation risks or the loss of therapeutic activity, requires that the basic coupled heat transfer and mass transfer phenomena, thermodynamic data (state diagram), and rheological properties should be analyzed in depth. Subsequently, the temperatures and the moisture levels, the temperature gradients, the moisture gradients and the shrinkage must be correctly controlled, not only during the freezing and the drying steps but also during the storage period following the lyophilization. Understanding and advanced modeling by physical laws of the coupled effects of the formulation parameters and the process conditions on these quality parameters constitute a large research field at the frontline of many basic disciplines that have to cooperate, on a scientific and rational basis, to solve the overall freeze-drying optimization problem. The scheme of Fig. 3.2 presents a

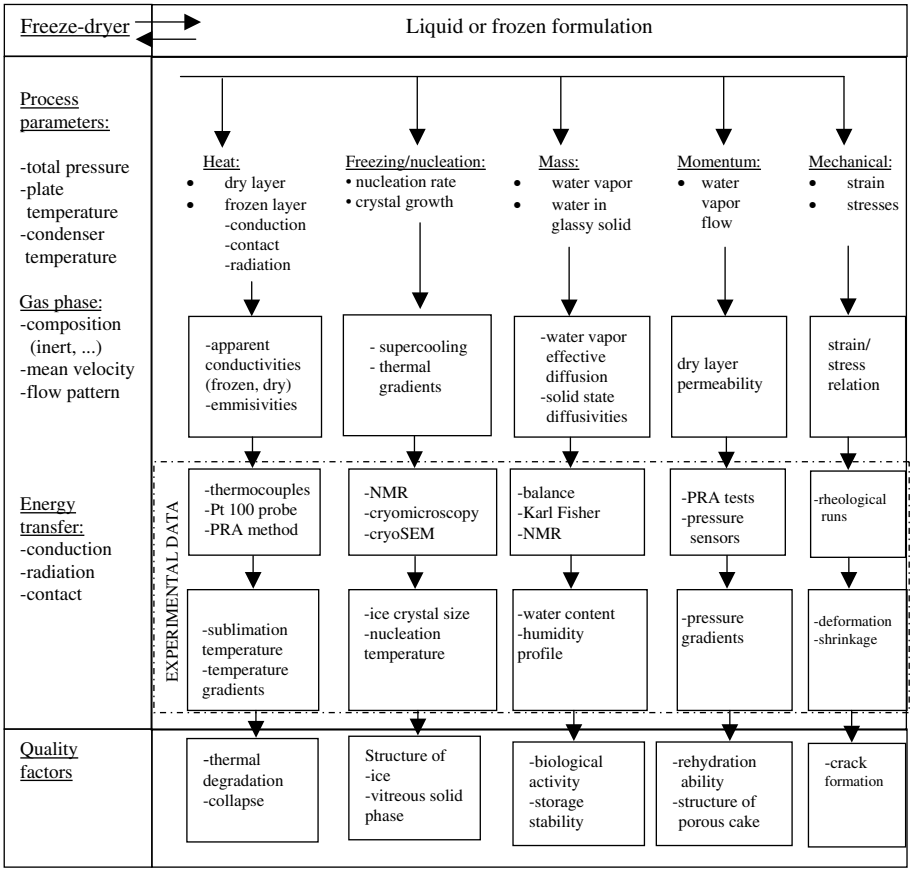

Fig. 3.2 A schematic representation of interactions between transport phenomena and quality factors during freeze-drying processes of pharmaceuticals.

synoptic view of the numerous interactions between transport phenomena and the main quality factors involved in drugs or in pharmaceuticals freeze-drying processes.

3.2.1
State Diagram, Melting Curves, Vitreous Transition, Collapse Temperature

Excipients or lyoprotectants are always added to the protein aqueous solution to maintain protein stability and its therapeutic or biological activity, first during the freezing step, next during the two drying steps – namely during the sublimation and desorption steps – and, finally, during the storage. This formulation step in the freeze-drying process development is a key step which is mostly realized by a trial and error approach, more often on a pure experimental and observation basis, without a clear knowledge of the individual action or the mutual interaction of each component. Respective "rules of the art" are generally available in the pharmaceutical industry and abundant literature has also been published (Pikal, 1990, 1992), but an analysis of these data is outside the scope of this chapter which is only devoted to the physical quality factors. Generally, the specialists agree that, if the formation of one amorphous or glassy phase and its upholding during the two drying steps is a necessary condition, in some cases, this condition is not sufficient to avoid the degradation reactions and to preserve the therapeutical protein activity. This is why the *state diagram*, which is very characteristic of the formulation composition, represents the *basic thermodynamical and physical data* absolutely necessary for setting up rationally the optimal freeze-drying cycle.

The state diagram for an amorphous system is presented in Fig. 3.3. If the freezing rate is not too rapid, after some supercooling preceding the nucleation step (A–B in the plot), the freezing process takes place at equilibrium along the liquidus curve (C–D in the plot) up to the glass transition temperature of the maximally concentrated solute, denoted T_g'. Then, a glassy solid phase appears where the active principle ingredient (API) – for example the therapeutical protein in the case of vaccines –

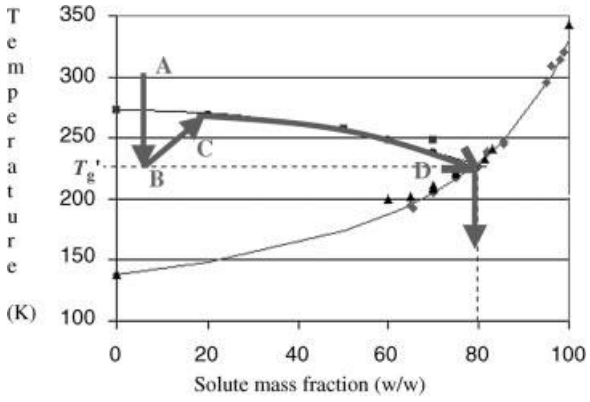

Fig. 3.3 Typical state diagram of a standard formulation used for freeze-drying of pharmaceutical proteins.

remains trapped in this amorphous phase. For a crystalline system without an amorphous solid phase, the whole solidification takes place at the eutectic temperature with possible formation of one (or various) solid solutions. Hereafter, we will list the main techniques commonly used to characterize and to optimize the principal quality factors of freeze-dried drugs or pharmaceuticals.

3.2.2
Characterization Methods: DSC, MDSC, Freeze-Drying Microscopy

The glass transition temperatures of the whole system are usually determined by differential scanning calorimetry (DSC) due to a significant change in the value of the heat capacity as the system passes from an amorphous state to a viscoelastic state accompanied by the formation of a significant peak at the glassy transition. Nevertheless, in some cases enthalpy relaxation effects may obscure the glass transition by overlapping peaks. Then, new DSC techniques such as "modulated" DSC (MDSC), which superimposes a nonlinear temperature variation on the linear temperature scan rate, are able to give a more efficient separation of the reversible effects coming from the increase in heat capacity at the glass transition from pure kinetic effects resulting from enthalpy recovery.

It is also possible to determine the *collapse temperature* of the formulation, which is another important characteristic parameter of the system, closely related to the glass transition temperature – generally a few degrees above – and that can be detected by freeze-drying microscopy and visual observation with a cryoscopy platform (Zhai *et al.*, 2003). This technique was originally reported by Mac Kenzie (1975) to be useful for identifying structural changes occurring during ice sublimation. The sample to be investigated is held between two glass covers on the cooling stage, cooled to approximately $-45\,^{\circ}C$ and then lyophilized as desired. At the location of the sublimation front, the state of the structure of the glassy matrix is evaluated visually. The collapse temperature is identified as the temperature at which this structure is observed to distort or to flow (formation of white zones on the microscopic images). Above the collapse temperature, the mechanical structure of the porous freeze-dried cake is destroyed. This identification is only an estimation since the collapse phenomenon (unlike melting) does not occur at a sharply defined temperature.

3.2.3
Ice Structure and Morphology: Cold Chamber Optical Microscopy

During the freeze-drying process, the freezing step is one of the most important steps because it fixes the structure and the physical properties of the frozen material and, consequently, it determines the final characteristics of the freeze-dried material morphology, its rehydration properties and its stability. The degree of supercooling determines the nucleation rates that is, the number of ice crystals and, therefore, the surface area and the mean size of the pores of the final freeze-dried matrix. For aqueous systems, high cooling rates lead to high supercooling degrees and to numerous small ice crystals. Consequently, small pores with a large surface area

are created; such pores present a low permeability for water vapor mass transfer. Conversely, low freezing rates give rise to bigger ice crystals and, consequently, to large pores in a freeze-dried matrix of higher permeability, which reduces the primary drying times but increases the secondary drying times (desorption) due to its small surface area, as shown experimentally by Kochs *et al.* (1993). Practically, heterogeneous nucleation takes place from microscopic impurities that are present in the solution or on the vial walls. Thus, individual vials are observed to nucleate in an apparently random fashion, some of them crystallizing slowly from the bottom of the vial, meanwhile in other vials nucleation is sudden all over the solution bulk. This can result in a large diversity of ice crystal structures, proving that the ice nucleation process is a complex stochastic phenomenon influenced by the composition (impurities) of the medium and by the cooling conditions that is, by supercooling and thermal gradients (Franks, 1990).

Searles *et al.* (2001a) and Nakagawa *et al.* (2006) confirmed in intensive and interesting studies conducted with glass vials and model formulations representative of pharmaceutical protein freeze-drying formulations the stochastic nature of the nucleation phenomenon, affected randomly by impurities or other heterogeneities. They also confirmed that the corresponding nucleation temperature was not under direct control. Furthermore, these authors observed for freeze-drying in vials of commercial size, that the experimental drying rates were directly related to the ice nucleation temperature and that cooling rates ranging from 0.05 to 1 $K\,min^{-1}$ had practically no effect on the nucleation temperatures and on the primary drying rates. They concluded that the nucleation temperature was the more relevant parameter in determining the structure of the ice crystals and the primary drying (sublimation) times. Thus, any nucleation temperature heterogeneities certainly result in large variabilities of all the other morphology-related parameters, such as the pore surface area of the freeze-dried matrix and the secondary drying (desorption or diffusion) rates. Consequently, factors such as impurities, particulate content, and vial conditions must be carefully controlled to avoid lot-to-lot variability during process development and scale-up. A freeze-drying cycle that was successful at the pilot scale could fail during large scale production if a rigorous control of these impurities is not achieved.

In the optimization of the freeze-drying processes, the ice crystal size must be large enough to obtain the shortest sublimation times during primary drying. However, during the secondary drying period (desorption), small ice crystals are favorable because they lead to a large specific surface area of the pores, promoting an easy desorption of water from the amorphous matrix. Consequently, to optimize the whole freezing-drying cycle, an optimal ice crystal size must be found. Such an optimal crystal size will minimize the total operating costs related principally to the duration of the drying steps.

In fact, concerning optimal freezing parameters, some authors, such as Pikal (1992) propose that a freezing protocol with moderate supercooling and rapid crystal growth could minimize the operating costs related to the total duration of the whole freeze-drying process and could present the lowest risks for protein damage at this process stage (aggregation, loss of structure, etc.).

Thus, many direct observation methods of the ice crystal structure for various frozen products have been used, such as cryo-scanning electron microscopy and nuclear magnetic resonance (Mahdjoub *et al.*, 2006). Otherwise, indirect methods like scanning electron microscopy (SEM) on freeze-dried sample can be used after sample freeze-drying. Cryo-fixation and cryo-substitution could also provide clear images but they have the disadvantage of partially destroying the sample (Berger and White, 1971; Woinet *et al.*, 1998). Patapoff and Overcashier (2002) developed a new interesting technique by introducing fluorescent dye to the formulation based on trehalose and by using a fluorescence microscope.

Furthermore, Chouvenc *et al.* (2006), Hottot *et al.* (2004), and Nakagawa *et al.* (2006, 2007a) set up and implemented for drug products a direct optical microscopy method in a cold chamber which had previously been used for analyzing the structure of the different phases of frozen foods (ice creams) (Caillet *et al.*, 2003). Then, these authors studied the influence of different freezing protocols and of annealing treatments on the size distribution of ice crystals for model and commercial frozen pharmaceutical formulations (see Section 3.3.1).This method is an optical microscopy method by reflexion with episcopic coaxial lighting which has the main advantage of best preserving the original structure of the frozen sample. When the freezing step was achieved, the vials were quenched into liquid nitrogen in order to stabilize the frozen structure and to maintain the sample below its glass transition temperature during its preparation. Sample handling and direct observation were performed inside a cold chamber at $-25\,^{\circ}C$. The samples are then carefully polished to obtain a smooth surface with roughness lower than $1\,\mu m$. In this manner, the sample could be observed directly in the cold chamber with a stereomicroscope (LEICA MZ12) equipped with a digital camera (Hitachi CCD) and with an optical fiber providing the episcopic coaxial lighting. A video monitor was placed inside the cold chamber in order to set up the different parts of the observation chain (lenses, etc.) during the adjustment procedure, but the PC used to store the pictures was located outside the cold chamber. Furthermore, all the optical parts were placed inside an airtight glove box to avoid possible water vapor condensation on the microscope lenses. During the observation, the frozen sample was maintained slightly above the T_g' value, but for a time short enough to avoid significant ice crystal size modification. Recorded images were analyzed with Visilog 5.4 software which allowed the estimation of the particle area and the equivalent diameter of the ice crystals.

3.2.4
Heat Flux Heterogeneity in the Sublimation Chamber

Because the heat flux is not evenly distributed through the sublimation chamber, resulting principally from the relative importance of the radiative flux component coming from the shelves and from the side-walls of the freeze-dryer, each vial of the whole batch does not receive the same overall heat flux. In fact, it is well known that the vials located at the edges of each shelf present shorter sublimation and desorption times and higher temperature profiles. This phenomenon can be investigated by

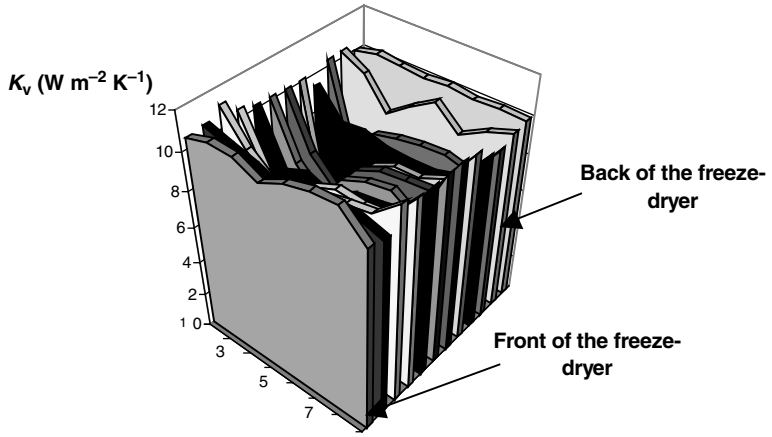

Fig. 3.4 Distribution of the values of the overall heat transfer coefficient for tubing vials of 7 ml according to Hottot *et al.* (2005); total pressure $P = 6$ Pa and shelf temperature $T = -5\,^{\circ}$C.

determining experimentally the sublimation rates with pure ice at different locations of the shelf, which allows one to set up a cartography of the overall heat transfer fluxes effective for the sublimation. Then, assuming the validity of the steady state sublimation hypothesis, these data allow the determination of an overall heat transfer coefficient, denoted by K_v. Figure 3.4 depicts the histogram of overall heat transfer coefficient values with respect to their location on the plate for tubing glass vials of commercial size (7 ml) and for standard freeze-drying conditions (total pressure, $P = 6$ Pa, shelf temperature $T = -5\,^{\circ}$C) obtained by Hottot *et al.* (2005) in a laboratory pilot freeze-dryer.

As a general rule, Hottot *et al.* (2005) observed that the vials located at the shelf center were subjected to 20% lower values of the heat transfer coefficient than those located near the edges of the plate, due to a strong heat flux heterogeneity on the plate of the freeze-dryer. As already pointed out, this nonuniformity of thermal fluxes received by each vial could be easily explained by the radiative effects which are dependent on the geometrical configuration and, consequently, vary with the position of the vial on the freeze-dryer plate. In this context, it is worth noting that, for a total gas pressure $P = 40$ Pa, the thermal conductance of the gas layer between the vial bottom and the shelf represents 50% of the total thermal conductance of the vial. This percentage varies largely with the total gas pressure from a highest value of 70% at $P = 80$ Pa, to a lowest value of 30% at $P = 6$ Pa. Consequently, for freeze-drying conditions at low total gas pressures, and due to the low thermal conductivities of gases in this region, an important part of the heat transfer resistance to the sublimation front is located in this thin gas layer between the vial bottom and the shelf.

Consequently, for the frequent situation of sublimation times controlled by the heat transfer, the reduction of the operating costs related to the drying time relies on the optimization of the thermal resistance by searching for an optimum of the total gas pressure or, if possible, by adapting the shape of the vial bottom. The latter can be done by reducing the space between the shelf and vial bottom as far as possible or by

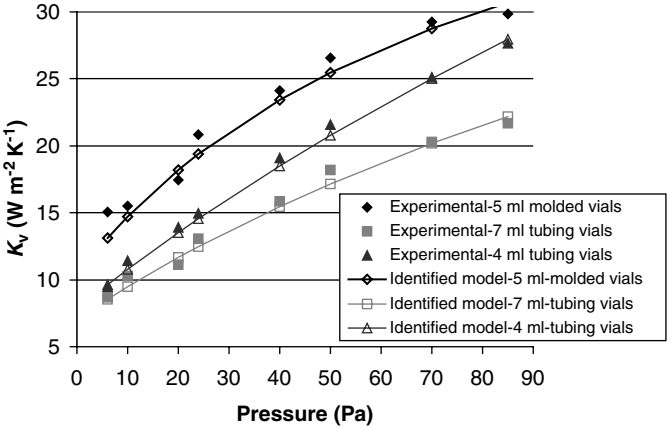

Fig. 3.5 Overall heat transfer coefficient as a function of total gas pressure for different types of vials, according to Hottot *et al.* (2005).

looking for other container geometries such as direct freeze-drying in syringe configuration, as proposed recently by Hottot *et al.* (2009a, b).

Furthermore, it is worth noting that the discussed heat transfer coefficient values are largely dependent on the vial type (molded or tubing), on the vial size, and also on the total gas pressure in the pressure range – between 10 and 70 Pa – usually selected for freeze-drying of sensible drugs (proteins, vaccines, etc.) (Pikal *et al.*, 1984).

Figure 3.5 represents the experimental and the correlated K_v values as a function of the total gas pressure for different vial types, obtained by Hottot *et al.* (2005).These curves show a clear, nonlinear dependance of the K_v values on the total gas pressure. Additionally, Fig. 3.5 shows that the heat transfer coefficient values are higher for the molded glass vials than for the tubing glass vials. This is also the reason why higher sublimation rates were found for the molded vials than for the tubing vials. Thus, each vial type and size has to be precisely investigated concerning its true thermal characteristics under the selected sublimation conditions (total gas pressure) in order to reach reliable and precise temperature profile predictions, for example for freeze-dryer control and monitoring purposes.

3.2.5
Permeability of Freeze-Drying Cake: Pressure Rise Tests

The pressure rise analysis method (PRA method), recently proposed by Chouvenc *et al.* (2004a), derived from the MTM method originally developed by Milton *et al.* (1997) and next modified by Obert (2001), appears to be a very promising noninvasive control method. It is a rapid, simple to implement and averaging tool that requires a freeze-dryer equipped with an external condenser and a very fast closing separating valve. The values of the main freeze-drying parameters, such as the temperature of the sublimation front, T_i, the resistance to water vapor mass transfer of the dried layer, R_p, and the overall heat transfer coefficient, K_v, could be

identified *in situ* and on line by fitting the experimental pressure rise data – obtained after the closing of the separating valve – with a physical model of the pressure response (PRA model). This method has also been proposed as a better way to determine the end of the primary drying period after which one can switch over to start the secondary drying period and increase the heating flux towards the bottom of the vial to activate the process of desorption of unfrozen bound water or the diffusion of water enclosed inside the vitreous solid solution.

If the freeze-drying process is controlled by water vapor mass transfer through the freeze-dried layer – for example in the case of dried cake of very low permeability or for very favorable heat transfer conditions – the drying rate for one vial is proportional to the mean driving force ($P_s - P_c$) – that is, to the water vapor pressure difference between the sublimation front interface and the drying chamber – and controlled by the freeze-dried cake mass transfer resistance, denoted R_p, which is inversely proportional to the dried layer permeability defined by Darcy's law. In this case it holds:

$$\dot{m} = \frac{P_s - P_c}{R_p} \tag{3.1}$$

Several techniques to determine experimentally the values of the freeze-dried cake mass transfer resistance, R_p, have been reported in the literature (Pikal, 1985; Patapoff *et al.*, 1999). They were all based on the gravimetric method used either for a single vial or for a limited number of vials. In contrast to such methods, the estimation of R_p values from the PRA model allows the determination of the mean freeze-dried product mass transfer resistance for the whole vial batch, averaging the heterogeneities of the cake structures between individual vials generated by the random nucleation phenomena. As shown in Fig. 3.6, a typical set of R_p values identified by the PRA model by

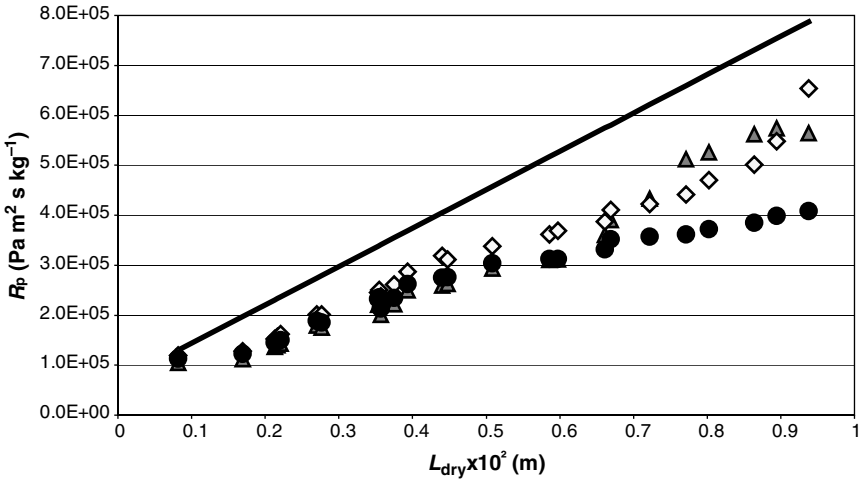

Fig. 3.6 Product resistance as a function of the thickness of the dry layer identified by the PRA model (diamonds), Milton's model (triangles), Obert's model (circles) and calculated from published data (Pikal *et al.*, 1985, solid line); Figure adapted from Chouvenc *et al.* (2004a).

Chouvenc *et al.* (2004a) was compared with the predictions of the two previously quoted MTM models. The position of the sublimation interface and the thickness of the dry layer, denoted L_{dry}, were estimated as functions of time by simple mass balances. Chouvenc *et al.* (2004a) observed that the R_p values derived from the three models were similar for $L_{dry} < 6$ mm and slightly lower than the few literature values. Moreover, experimental data correlation lines pass close to the axis origin, so that no significant crust effect was present in the experimentally investigated crystalline system (mannitol), in contrast to what is observed with concentrated vitreous systems that can present relatively large crust effects.

3.2.6
Estimation of Mean Product Temperature

It is important for the control of the freeze-drying process to have a precise and rapid estimation of the mean product temperature in order to maintain this temperature as high as possible during the sublimation period without going beyond the T_g' value or without overshooting the collapse temperature during the secondary drying period. As pointed out by many authors (Pikal, 1990, 1992), it is worth noting that this physical parameter is the key parameter for the control of numerous quality factors of the final product.

Insertion of thermocouples or Pt 100 sensors in a few vials is a widely used method to measure the mean product temperature. Nevertheless, it is well known that this sensor insertion modifies notably the elementary phenomena of nucleation and of ice crystal growth, by lowering the degree of supercooling which leads to an increase in the average ice crystal size in the frozen matrix. As a consequence, the mass transfer resistance to water vapor flux through the dried layer in monitored vials is considerably reduced. Moreover, these monitored vials, for technical reasons, are usually placed close to the loading door and, thereby, submitted to wall and radiative effects. All these reasons tend to make the monitored vials dry faster, preventing them from being representative of the entire vial batch. Furthermore, this method is based on a manual procedure that may compromise product sterility when manufacturing sterile pharmaceutical products such as vaccines.

Recently, Chouvenc *et al.* (2004a) published a comparative and critical study of the MTM models with their own new physical model, the PRA model, allowing the estimation of the values of some key parameters of the freeze-drying process such as the ice sublimation front temperature, the mass transfer resistance of the dried layer and the overall heat transfer coefficient of the vial. The estimated ice front temperature values from the previously mentioned models are compared in Fig. 3.7 with experimental data obtained from vial bottom temperature measurements conducted with thin thermocouples during freeze-drying runs in the case of glass tubing vials with 5% w/w mannitol solutions. Chouvenc *et al.* (2004a) observed that the temperature values identified by the three models are quite close to the experimental ones even though estimated temperatures during the primary drying period were systematically 1–3 °C higher than the experimental ones (thermocouples). This difference was inversed during the second half of the primary drying period due to artefacts

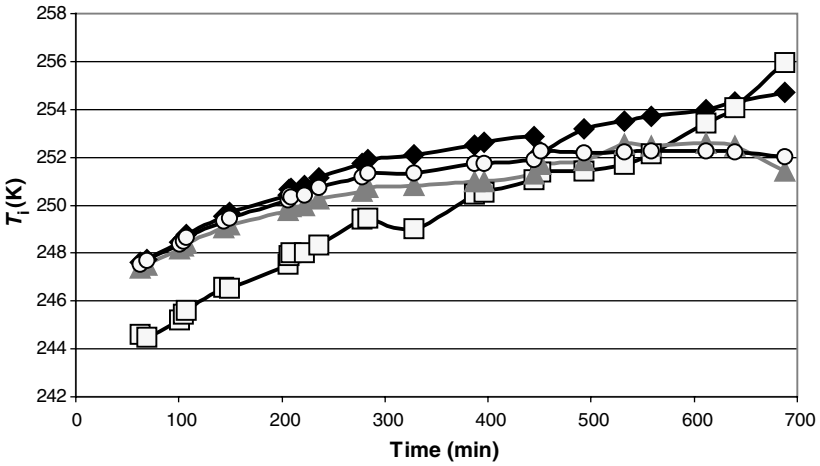

Fig. 3.7 Ice sublimation front temperature: Comparison between PRA model (diamonds), Milton's model (triangles), Obert's model (circles) and mean product temperatures (squares) measured by thermocouples; (Chouvenc *et al.*, 2004a).

of the PRA model itself when the sublimation surface area is no longer constant due to the heat flux heterogeneities on the plate of the freeze-dryer.

Consequently, the PRA method for non-invasive temperature estimation seems to be quite reliable during the first half of the primary drying period and thus allows an efficient on-line and *in situ* control of the mean product temperature. Nevertheless, due to possible reduction in the sublimation surface at the end of the primary drying period, all the models tend to underestimate the sublimation temperature so that, for thermosensible products like therapeutic proteins, extreme caution should be taken when using this method during this primary drying end period.

Recently, a new sensor that enables wireless product temperature measurement has been proposed and is under commercial development. This sensor, that can be sterilized, receives its power by excitation of a passive transponder through a radio-frequency field (2.4 GHz, ISM band). The signal analysis gives the temperature at the bottom center of the vial in real-time without any heat conduction effects to the product (Schneid and Gieseler, 2008). Nevertheless, Schneid and Gieseler have observed that the positioning of the sensor in a given vial with respect to the bottom center was crucial in order to obtain reliable temperature profiles and, consequently, for an adequate monitoring of the primary drying step end-point.

The water vapor pressure, that is, the gas relative humidity, in the drying chamber is mostly fixed by the condenser temperature so that this process parameter can also be used, in parallel with the shelf temperature, to avoid quality losses due to overdrying by adjusting the most adequate relative humidity in the sublimation chamber. During the secondary drying period (desorption or diffusion period), the drying rate gradually decreases as soon as the process becomes more and more controlled by the diffusion of the water inside the amorphous solid (Pikal, 1992). Moreover, the glass transition temperature of the material increases as the drying

proceeds so that the product temperature can be regularly increased while being maintained below the glass transition temperature or the collapse temperature to avoid the collapse of the porous layer structure (Bardot *et al.*, 1993; Roy *et al.*, 1989).

Additionally, many experimental studies have shown that, for various protein systems, the storage stability improves as the residual humidity decreases and that the optimal final water content is generally around 1% or less. Water contents above the monolayer content increase the mobility of the water that becomes more available for protein degradation reactions with the other solutes of the concentrated phase. Moreover, water is a plasticizer of the amorphous phase that decreases the T_g value, which leads to more difficult storage conditions. Finally, it should be noted that the moisture content is generally not uniform within the vial, the top and the wall zones of the cake being the driest zones and these non-uniformities in the spatial distribution of the water content generally increase with the size of the vial.

3.3
Influence of Freezing and Freeze-Drying Parameters on Physical Quality Factors

This section is devoted to the discussion and analysis of typical data showing the influence of the freezing and freeze-drying parameters on the main physical quality factors encountered during freeze-drying of drugs.

3.3.1
Influence of Freezing Protocol on Ice Morphology

During the freeze-drying process, the freezing step is one of the most important steps because it fixes the structure and the morphology of the frozen material and, consequently, it determines the final morphology of the freeze-dried material and thus its rehydration properties and its stability. During this step, the interdependent phenomena of supercooling, ice nucleation and ice crystal growth that take place successively are directly related to the cooling rate and to the thermal gradients in the supercooled solution. Thus, the degree of supercooling determines the nucleation rates that is, the number of ice crystals formed and, consequently, the surface area and the mean size of the pores of the final freeze-dried matrix. High cooling rates lead to high supercooling degrees, to numerous small ice crystals and, eventually, to small pores with a large surface area that have a low permeability to water vapor mass transfer. Conversely, low freezing rates give bigger ice crystals and, consequently, large pores in the freeze-dried matrix of higher permeability, which reduce the primary drying times but increase the secondary drying times (desorption) due to their small surface area.

Patapoff and Overcashier (2002) have reported three types of freezing protocols used during lyophilization processes, namely:

- Fast freezing by immersing the vials rapidly into the cooling bath; in this case it proved that the nuclei were formed first at the walls of the vial, next at the vial bottom and finally in the center and at the top of the vial.

- Vertical freezing obtained by cooling the solutions with wet ice, with nucleation triggered at the vial bottom with dry-ice, and then placing the vials on a shelf cooled at −50 °C; the ice crystals grow vertically, without any skin effect on the cake surface. This freezing type leads to large ice crystals.
- Standard freezing by placing the vial on the precooled shelf; after the solution enters the supercooling state, for standard cooling rates, the spontaneous nucleation process starts at the vial bottom and then the crystals grow vertically.

For all these freezing types, a more or less complex ice morphology was usually observed, depending principally on three governing interdependent freezing parameters, namely the cooling rate, the supercooling degree and the ice nucleation temperature.

In extensive and interesting studies with glass vials and model formulations representative of pharmaceutical protein freeze-drying formulations, Searles *et al.* (2001a) and Nakagawa *et al.* (2006) confirmed the stochastic nature of nucleation phenomena which were affected randomly by impurities or other heterogeneities. Thus, they concluded that the nucleation temperature, which is a non-deterministic parameter, is, nevertheless, the more relevant parameter that determines the ice crystal structure and the primary drying times. Moreover, nucleation temperature distributions generally observed between different vials in pilot and laboratory scale equipment certainly result in large variability of all other related morphological parameters, such as the pore surface area of the freeze-dried matrix, and the primary and secondary drying times.

It was observed by Hottot *et al.* (2006a) that the size distributions of the ice crystals depend not only on the freezing rate but also on the vial size and type, and on the filling height. For example, molded vials or higher values of vial filling height reduce the heterogeneities of morphology resulting from variability of the supercooling degree and allow one to obtain more homogeneous ice crystal size distributions (cf. Section 3.3.1.2). This behavior was explained by the decrease in the supercooling effect which generally leads to broad and non-homogenous distributions of ice crystal morphology. Consequently, such factors as impurities, particulate content, vial geometry and type, filling height, and so on must be carefully controlled to avoid lot-to-lot variability during industrial process development and scale-up.

3.3.1.1 **Influence of Freezing Rate**

The experimental data of Fig. 3.8 obtained by Hottot *et al.* (2004) compare the cumulative distribution of ice crystal size for different freezing protocols and for different aqueous model formulations, close to drug formulations processed in practice by freeze-drying. It is clearly confirmed that the ice crystal size decreases when the freezing rate increases, see, for example, the data gained by cooling with liquid nitrogen. The same effect has been previously observed during model food freeze-processing by Faydi *et al.* (2001).

Consequently, the cooling rate has a large influence on the ice crystal morphology and it is also the easiest freezing operating parameter to control experimentally that greatly influences this ice crystal morphology. This is why the influence of the cooling

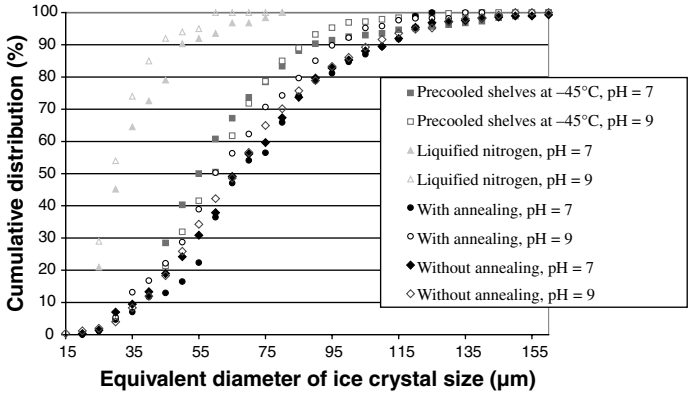

Fig. 3.8 Cumulative distributions of ice crystal size. Influence of freezing protocol and formulation (BSA based) according to Hottot *et al.* (2004).

rate on ice crystal size and dried layer permeability was simulated by a semi-empirical model as a function of nucleation temperature by Nakagawa *et al.* (2007a). The simulation data presented in Fig. 3.9 clearly show that an increase in cooling rate leads to smaller ice crystal sizes, as also observed experimentally. It is noteworthy that this tendency becomes much more pronounced by increasing the nucleation temperature, so that the dependence of the ice crystal size on the nucleation temperature becomes much greater by decreasing the cooling rate. On the contrary, when samples are prepared at high cooling rates equal to $-5\ \mathrm{K\,min^{-1}}$ (fast cooling), the variation in nucleation temperature does not have too large an influence on the mean size of the ice crystals. Consequently, ice morphologies obtained under such

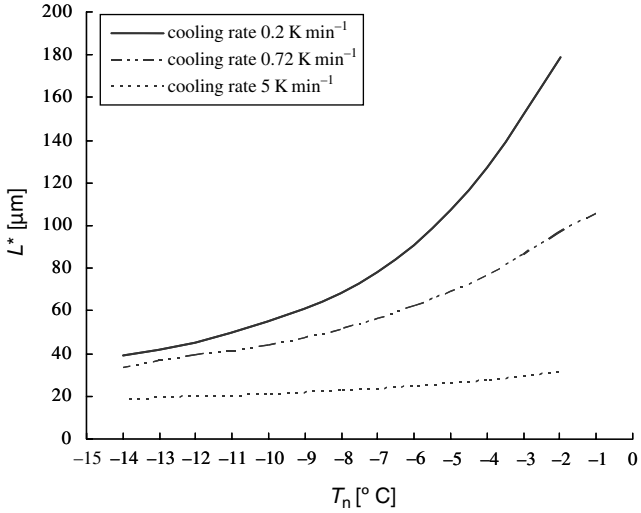

Fig. 3.9 Simulation of the influence of cooling rate on ice crystal mean size (mannitol) according to Nakagawa *et al.* (2007a).

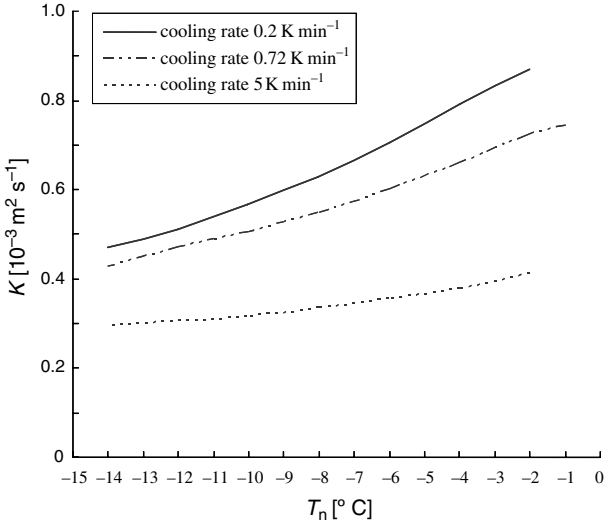

Fig. 3.10 Simulation of the influence of cooling rate on dried layer permeability according to Nakagawa *et al.* (2007a).

conditions result in relatively uniform sublimation rates during subsequent drying steps.

Values of the permeabilities of the freeze-dried layer derived from the previously mentioned modeling are presented in Fig. 3.10. They clearly explain the well known influence of the freezing protocol – more precisely of the nucleation temperature – on the duration of the subsequent sublimation step as also observed experimentally (compare with Section 3.3.1.2).

3.3.1.2 Influence of Vial Type and Filling Height

In order to properly observe the influence of vial type and size, Hottot *et al.* (2006a) filled the vials with different solution volumes to maintain the same initial height of solution at the beginning of the freezing step, namely $h = 6.7$ mm. The distribution curves of the ice crystal diameters obtained for a standard freezing protocol are presented in Fig. 3.11.

The reported distribution curves represent all data gained by cutting frozen formulations at three different levels, namely at the top, the middle and the bottom of the frozen sample. The authors observed that the mean ice crystal diameters were larger for 7 and 5 ml vials than for 4 ml vials and that the distributions were rather equal for 5 and 7 ml vials (Hottot *et al.*, 2006a).

The filling height for a given vial size is also an interesting parameter to investigate as it influences significantly the thermal gradient inside the solution, that is, the supercooling degree and the nucleation rate. The data obtained by Hottot *et al.* (2006a) for 4 ml tubing vials are presented in Fig. 3.12 and show a significant increase in mean ice crystal diameter values, from 20 to 10 μm, when the initial filling height increased from 6.7 to 10 mm, all other freezing parameters being constant.

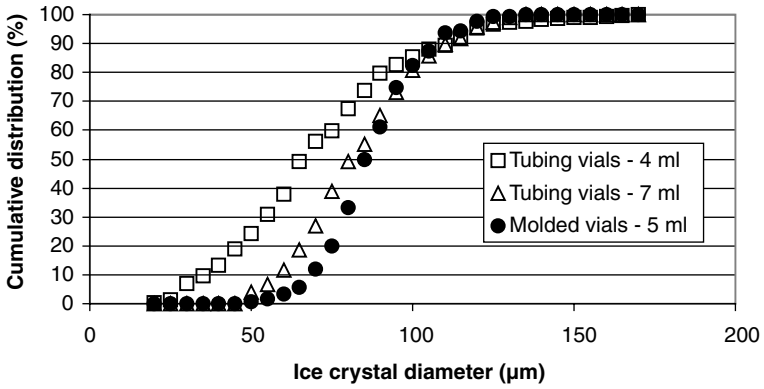

Fig. 3.11 Cumulative distribution of ice crystal size for different types and sizes of vials; $h = 6.7$ mm, cooling rate: $-0.6\ \mathrm{K\,min^{-1}}$ (Hottot *et al.*, 2006a).

These authors also determined the supercooling degrees by sticking thin thermocouples onto the exterior surface of the vial bottoms. These non-invasive temperature measurements showed clearly that an increase in the initial filling height of the vial corresponds to lower supercooling degrees, and, consequently, to lower nucleation rates. Therefore, it finally leads to higher mean ice crystal sizes and to coarser ice phase structures.

3.3.1.3 **Annealing**

In some cases, heat treatment, called annealing, is applied after the freezing step and before the two drying steps for homogenization of the ice crystal structure and, thus, for obtaining a more uniform and more permeable dry cake structure. It consists in

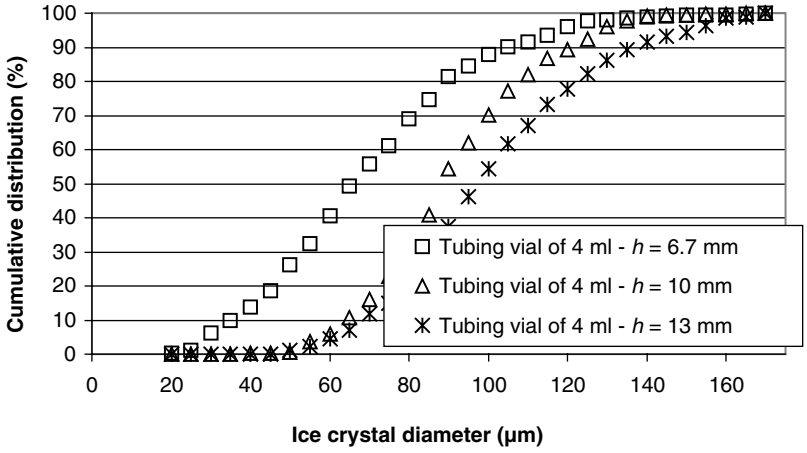

Fig. 3.12 Influence of filling height on the cumulative distribution of ice crystal size, tubing vials of 4 ml, cooling rate: $-0.6\ \mathrm{K\,min^{-1}}$. (Hottot *et al.*, 2006a).

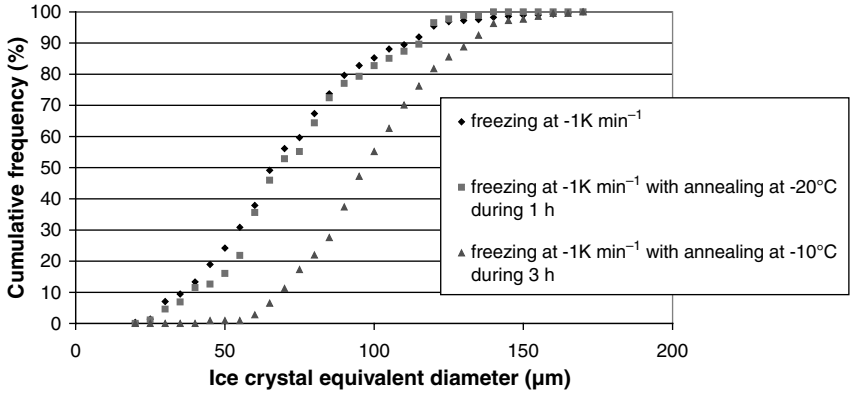

Fig. 3.13 Ice crystal size distribution, influence of annealing parameters (Hottot *et al.*, 2004).

increasing the temperature of the frozen system to some value between the vitreous transition temperature and the melting temperature for a certain duration, so that, by recrystallization, the smaller crystals produced by rapid cooling (high nucleation rates) disappear to form larger ice crystals (Fig. 3.13).

It is well known that annealing, which is a thermal treatment applied to the product above its glass transition temperature right after the initial freezing step, allows an increase in the sublimation rates by increasing the mean size of ice crystals in the frozen matrix (see Fig. 3.14) leading to lower values of the resistance to mass transfer of water vapor of the dried layer, R_p (Searles *et al.*, 2001b; Chouvenc *et al.*, 2006; Hottot *et al.*, 2008). Another benefit discovered by the same authors is that annealing also homogenizes inter-vial sublimation kinetics from one vial to another throughout a whole batch. However, the desorption kinetics of unfrozen water, which was proved to be proportional to the specific surface area of the freeze-dried product (Pikal, 1990), is expected to decrease by increasing the mean ice crystal size and, thus, decreasing the surface area of the pores generated by the sublimation step.

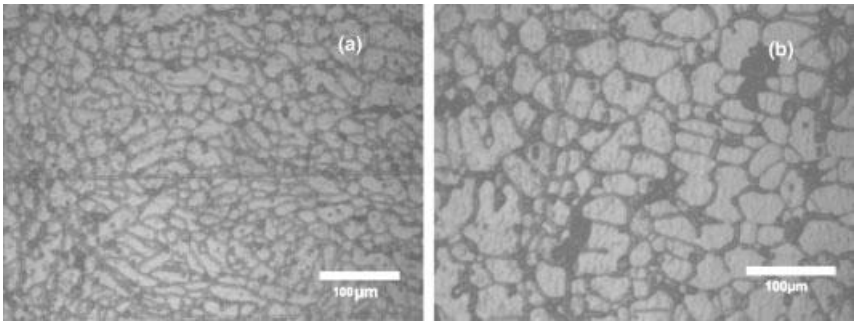

Fig. 3.14 Examples of images obtained at the middle of the sample, (a) before and (b) after 30 min of annealing at −10 °C (Chouvenc *et al.*, 2006).

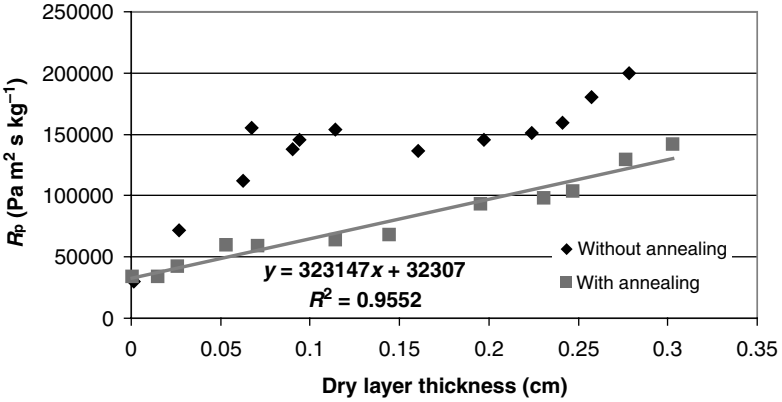

Fig. 3.15 Resistance to water vapor mass transfer as a function of dry layer thickness with and without annealing (Chouvenc *et al.*, 2004a).

Chouvenc *et al.* (2004a) implemented the pressure rise test method with the PRA model to identify the freeze-dried layer mass transfer resistance, denoted by R_p, as a function of time and to obtain the values of sublimation front temperature during freeze-drying cycles with or without annealing. These authors observed that, after the first 30 min necessary to reach the quasi-steady state of the primary desiccation period, the annealing treatment enabled them to decrease the product temperature by about 2 °C for the same operating conditions of sublimation. Furthermore, this decreasing tendency was also observed on the R_p values obtained, the annealing treatment decreasing by more than 50% the R_p values after the first 5 h of sublimation, corresponding to a dry layer thickness $L < 0.35$ cm (see Fig. 3.15). Moreover, without annealing treatment, the R_p values rose rapidly and then stabilized after 3 h of sublimation. This behavior could be due to the presence of small ice crystals near the external surface of the sample, leading to significant mass transfer resistance in this zone. The structural heterogeneity of the frozen matrix observed by direct microscopy confirmed this hypothesis. One additional feature of the data of Fig. 3.15 is that the mass transfer resistance value obtained by extrapolation to zero dried layer thickness has a value equal to 32 kPa m^2 s kg^{-1}, which certainly indicates the formation of a crust at the superior surface of the dry layer. The effect of crust formation was confirmed by Mahdjoub *et al.* (2006) by using MRI (magnetic resonance imaging). These various results prove that adequate annealing treatments – as far as duration and temperature levels are concerned – increase significantly the ice crystal mean size (Ostwald ripening), improve the water vapor mass transfer permeability and, consequently, reduce the primary drying times. This last effect, certainly due to a rearrangement and to a uniformization of the ice crystal structure strongly increases with the temperature and the duration of the annealing treatment (Hottot *et al.*, 2005; Chouvenc *et al.*, 2006). Generally, different authors also implemented different and complementary characterization methods in order to quantify the impact of annealing on key freeze-drying parameters such as ice crystal mean sizes, sublimation rates and desorption kinetics (Searles *et al.*, 2001b; Hottot *et al.*, 2004).

3.3.2 Controlled Nucleation

Different methods can be implemented for triggering the nucleation process and reducing the effect of the rather broad distribution of spontaneous nucleation temperature which is one of the main causes of vial-to-vial variation of ice morphology and, consequently, of the distribution of drying times and of distributed morphology parameters in the freeze-dried product.

Among these methods, the "ice fog method" consists in producing a vapor suspension of small ice crystals by contact of a cold gas with the humid atmosphere of the sublimation chamber of the freeze-dryer and by using these ice crystals as nucleating agents when they contact the surface of the subcooled solution. Rambhatla *et al.* (2004) investigated, in a recent study with model solutions of different saccharides, the effect of nucleation temperature on the primary drying process by using this ice-fog induced nucleation to control the nucleation process. They observed that the specific surface area of the freeze-dried cake increased with decreasing nucleation temperature, whereas the water vapor mass transfer resistance increased with increasing specific surface area of the cake. Thus, the morphology of the dried cake (pore surface area and freeze-dried cake permeability) proved to be rather well correlated with the degree of supercooling and with the subsequent nucleation temperatures.

Nevertheless, the main drawback of this method is that the distribution of the small ice crystals can be non-uniform along each plate of the freeze-dryer due to a complex and uncontrolled gas flow regime in the interior of the sublimation chamber.

Among other methods to trigger the nucleation by application of an external energy field to the supercooled solution, the application of a high voltage electric field has been investigated recently by Petersen *et al.* (2006). These authors reported that the structure and morphology of the ice crystals are greatly dependent on the freezing parameters that determine the rate of the freezing front. They also reported that the sublimation rate is strongly related to the ice morphology, the mean sublimation times being reduced by about 30% if the cooling rate during the freezing step is lowered by 1 K min^{-1}. Additionally, some authors have recently studied the method of using power ultrasound to control the nucleation temperature at predetermined values; in the following section, we will analyze and summarize their principal results (Morris *et al.*, 2004; Nakagawa *et al.*, 2006; Saclier *et al.*, 2008).

3.3.2.1 Controlled Nucleation by Ultrasound Sonication

It is well known that supercooled solutions without any nucleation control start their nucleation quite randomly so that, for the same cooling rates and the same experimental conditions, the nucleation temperatures are widely distributed. This behavior was observed by Nakagawa *et al.* (2006), as shown in Fig. 3.16 where the frequency distributions of experimental spontaneous nucleation temperatures are presented for mannitol, BSA and sucrose systems frozen at the same standard cooling rate, -1.0 K min^{-1}. All plotted data were obtained under similar and rigorously controlled cooling conditions (cooling rates) and with glass vials (type, size, etc.) as clean and

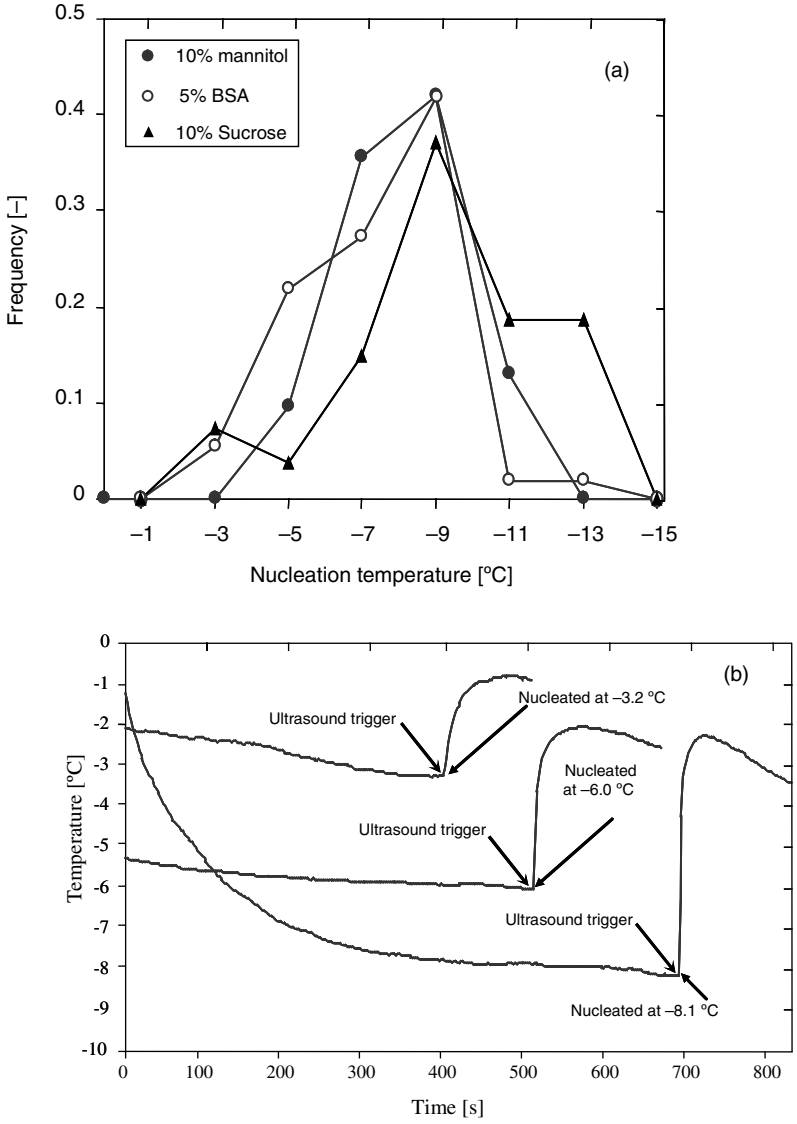

Fig. 3.16 (a) Frequency distributions of spontaneous nucleation temperatures and (b) thermograms with ultrasound triggered nucleation, at freezing rates equal to $-1\,\mathrm{K\,min^{-1}}$ with tubing vials of 3 ml (Verretubex) (Nakagawa *et al.*, 2006).

identical as possible. The authors observed that the nucleation temperatures varied from -2 to $-15\,^{\circ}\mathrm{C}$ for all the investigated standard systems with an average value around $-8\,^{\circ}\mathrm{C}$. The application of ultrasound power (in the range from 30 to 40 kHz) to supercooled aqueous solutions was used by Nakagawa *et al.* (2006) to control the nucleation processes at selected temperatures. The main mechanism that triggers nucleation by ultrasound, according to Hickling (1965), is based on acoustic cavitation,

which produces small gas bubbles that grow rapidly and then collapse generating locally very high transient pressure fields that trigger the formation of the first nuclei. This technique has been implemented experimentally by different authors for pure water or for dilute aqueous solutions (Chow *et al.*, 2003, 2005; Inada *et al.*, 2001; Zhang *et al.*, 2001, 2003). These authors observed that the acoustic power and the gas bubble concentration within the solution are the key nucleation parameters; when the values of these two parameters increase, the nucleation induction time decreases. A physical model was recently developed by Saclier *et al.* (2008) to predict the number of nuclei generated (i.e., the nucleation rate) first by a single gas bubble and, next, by a multi-bubble system as a function of the acoustic pressure (ultrasound amplitude) and the supercooling degree (supercooled liquid temperature). The predicted nucleation rates were found to increase by increasing the degree of supercooling and the ultrasound power (i.e., the acoustic pressure) in good agreement with the previously published experimental data. Because ultrasound provides a non-invasive method to control the ice morphology during static freezing in vial configuration and, consequently, to also control the morphology of the freeze-dried product, this method has been used recently in several projects with the goal of developing new freeze-drying technologies, for example, by Morris *et al.* (2004). At nucleation temperatures close to the melting point, they observed that the closer the nucleation temperatures to the melting point, the larger the mean size of the ice crystals obtained. They also observed that the application of ultrasound triggering reduces the morphological heterogeneities of the dried layer to water vapor flow.

3.3.2.2 Effect of Ultrasound on Structural and Morphological Properties

A nucleation control system using ultrasound, which allows coupling of the cooling step with ultrasound wave propagation, was set up and described in detail by Nakagawa *et al.* (2006). They were able to trigger the nucleation process of the supercooled solution contained in 3 ml tubing glass vials (Verretubex) at selected and predetermined values of temperature with a high degree of repeatability, provided that a convenient mechanical and thermal contact between the vial bottoms and the cooling plate could be achieved. Ice crystal structures obtained from 10% mannitol frozen solutions were directly observed by optical microscopy in a cold chamber. The observed surfaces were vertical and horizontal sample cuts that corresponded to a cross-section of the cylindrical frozen sample. Some selected images that represent the more typical trends of each sample are shown in Fig. 3.17 (vertical cross-sections). In these images, the ice crystals appear in white and the cryoconcentrated phase, corresponding to mannitol crystals, in black. These images show clear morphology differences of the ice crystals depending on their nucleation temperatures. Thus, large and directional ice crystals (dendrite type) were observed with the sample nucleated at higher temperature (i.e., at lower supercooling degree), while small and numerous ice crystals were observed with the sample nucleated at lower temperature (i.e., with higher supercooling degree). Ice crystal nucleation and growth generally start from the bottom to the top of the vial, and simultaneously a highly cryoconcentrated solution layer appears at the vial top. Thus, it was also confirmed on these vertical cut images (Fig. 3.17) that the ice crystal nucleation triggered by the

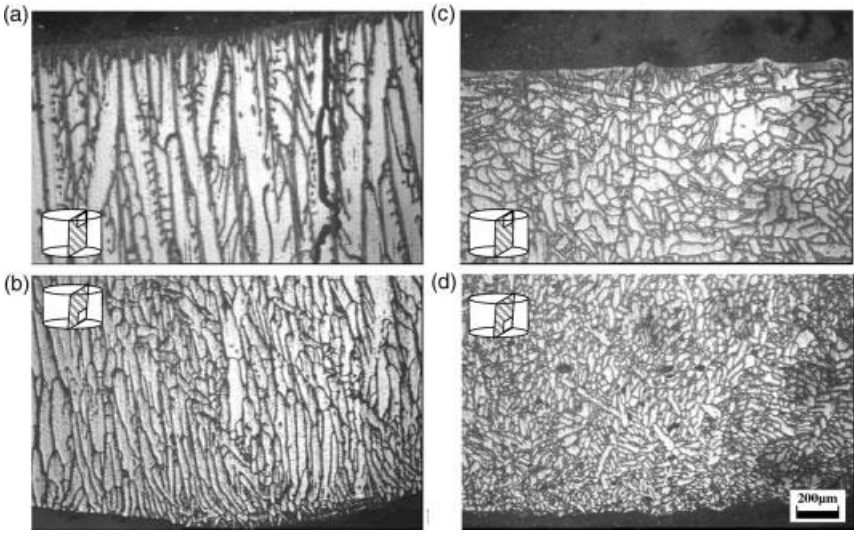

Fig. 3.17 Ice crystal structures on vertical cross-sections (10% mannitol); (a) upper position, nucleated at −2.04 °C, (b) lower position, nucleated at −2.04 °C, (c) upper position, nucleated at −8.17 °C, (d) lower position, nucleated at −8.17 °C according to Nakagawa *et al.* (2006).

ultrasound waves occurred at the vial bottom because one can observe smaller ice crystals at the vial bottom than at the vial top. This observation also means that the growth of ice crystals nucleated by ultrasound progresses in the same manner as in the case of spontaneous nucleation. This hypothesis was also confirmed by Nakagawa *et al.* (2006) who observed the same values of average ice crystal size by comparing the ice crystal morphology of samples nucleated by ultrasound and samples nucleated spontaneously at the same temperature.

3.3.3
Relationship between Nucleation Temperatures and Sublimation Rates

Overall primary drying rate values were determined gravimetrically for 10% mannitol solution by Nakagawa *et al.* (2006) and the corresponding values are plotted as a function of nucleation temperatures in Fig. 3.18. These data show a rough proportionality relationship between the primary sublimation rates and nucleation temperatures and confim the previous data published by Searles *et al.* (2001a). For this standard formulation that is largely used for drugs freeze-drying, the sublimation rates were approximately doubled by increasing the nucleation temperature from −8 to −2 °C by ultrasound nucleation control. In the case of freeze-drying of 5% BSA samples, the achieved enhancement of sublimation rates was lower, even if the average values of the sublimation rates were higher than for other investigated formulations (Nakagawa *et al.*, 2006).

It is also worth noting that the sublimation rates of samples that nucleated spontaneously are located on the same line as those corresponding to controlled

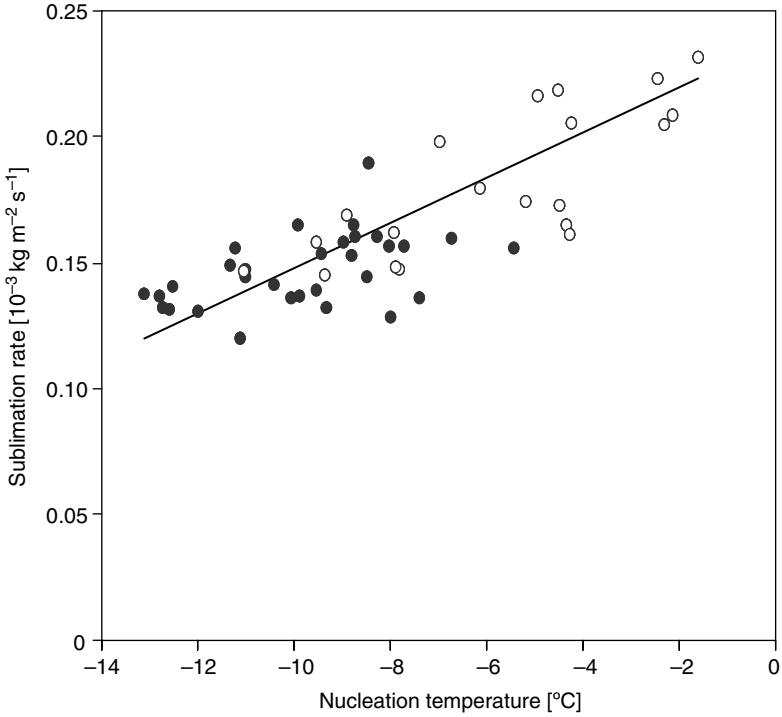

Fig. 3.18 Primary drying rates versus nucleation temperatures; open symbols: controlled nucleation by ultrasound, closed symbols: spontaneous nucleation (10% mannitol) according to Nakagawa *et al.* (2006).

nucleation samples in Fig. 3.18. This observation confirms the hypothesis that the mechanisms of ice crystal growth in the samples nucleated by ultrasound are equivalent to the mechanisms prevailing in the samples that nucleated spontaneously.

In this way, it could be demonstrated that the morphological parameters of ice crystals of frozen formulations are strongly related to nucleation temperatures, which finally fixes the permeability of the freeze-dried matrix. These data confirm the adequacy of ultrasound systems for controlling the nucleation step and, in consequence, for accelerating notably the primary sublimation rates during the freeze-drying process of pharmaceuticals in vials and, finally, for reducing the operating costs related to drying times, Hottot *et al.* (2005, 2006a); (Nakagawa *et al.*, (2007b).

3.3.4
Freeze-Dried Cake Morphology

3.3.4.1 Water Vapor Mass Transfer Resistance

Since the water vapor pressure increases exponentially with the temperature, the drying rates during freeze-drying processes, which vary in a similar way, are strongly dependent on the sublimation front temperatures that is, on the shelf temperature.

Otherwise, as already emphasized in Section 3.3.3, for a given formulation, the water vapor mass transfer resistance values are directly dependent on the pore morphology of the freeze-dried zone, and, consequently, on the ice crystal morphology, that is to say on the freezing conditions and on the thickness of the freeze-dried layer which increases throughout the sublimation step.

The mass transfer resistance of water vapor in the freeze-dried layer can be estimated from the molecular diffusion laws in the Knudsen regime, which corresponds usually to the experimental conditions encountered during standard freeze-drying of fragile pharmaceutical proteins (the value of the Knudsen number is quite commonly higher than 2). In order to model water vapor mass transfer Hottot *et al.* (2005, 2006b) assumed that the mean pore size was equal to the mean diameter of the ice crystals. These latter values were determined by direct optical microscopy in a cold chamber from image analysis of frozen formulation cuts, or estimated by the semi-empirical modeling approach by Nakagawa *et al.* (2007a). Owing to the definition of R_p (Eq. 3.1) and to the laws of molecular diffusion in the Knudsen regime, the theoretical expression for R_p becomes:

$$R_p = R_p(L_{dry} \to 0) + \frac{1.5 L_{dry}}{\bar{d}_{pore}} \frac{\tau}{\varepsilon} \sqrt{\frac{\pi \tilde{R} T}{2 \tilde{M}_w}} \tag{3.2}$$

where R_p ($L_{dry} \to 0$) is the limiting value of the water vapor mass transfer resistance when the dried matter layer thickness tends to zero; τ is the tortuosity factor, ε is the porosity of the freeze-dried cake (equal to the water volume fraction), T is the mean product temperature (K), $\bar{d}_{pore}$ is the mean pore diameter, and L_{dry} the freeze-dried layer thickness.

This relationship for the Knudsen regime (low total gas pressure, low sublimation temperature) has been validated by Hottot *et al.* (2005) who compared with freeze-drying experiments conducted with a model BSA formulation with annealing treatment (cf. Fig. 3.19). In the case of a standard freeze-drying cycle, this successful validation represents a positive result due to numerous assumptions involved in the model and to quite large uncertainties in the corresponding model parameter values.

Thus, for $L_{dry} < 3$ mm, the experimental values of the water vapor resistance were well predicted by the above mass transfer model, as Fig. 3.19 shows. However, for dried layer thicknesses of $L_{dry} > 3$ mm, the curve $R_p = f(L_{dry})$ was no longer linear. This point corresponds to the limit beyond which the total sublimation area inside the vials certainly decreases (wall effect due to radiation flux). Nevertheless, the same authors observed that, without annealing treatment, the experimental values of R_p could not be predicted so accurately by the same model. This discrepancy possibly results from wider ice crystal size distributions in samples without annealing. A significant homogenization of morphology certainly occurred in the case of cycles with annealing, leading to more uniform pore sizes all through the bulk of the freeze-dried matrix which is in accordance with the hypothesis of Eq. 3.2. Moreover, for standard formulations used industrially in vaccine freeze-drying, Chouvenc *et al.* (2004b) observed that the mass transfer resistance values increased more or less monotonically as a function of the dried layer thickness, and that an annealing

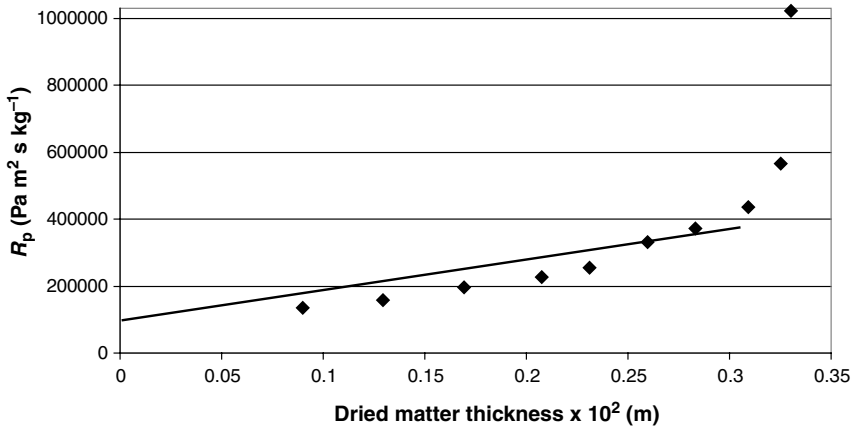

Fig. 3.19 Water vapor mass transfer resistance versus freeze-dried layer thickness. Continuous line = model prediction, according to Hottot *et al.* (2005).

treatment after the freezing step was an efficient method to homogenize and improve the permeability of the dried zone, thus reducing the primary drying times.

3.3.4.2 Freeze-Dried Layer Permeability

The concept of permeability introduces another overall parameter often used to characterize globally the morphology of porous media with respect to gas flow. Thus, for interpreting the sublimation data during freeze-drying processes, the water vapor permeability, denoted by K, is classically defined by the following relationship (Darcy's law):

$$\dot{m} = \frac{K\tilde{M}_w}{\tilde{R}T}\mathrm{grad}P \tag{3.3}$$

Equation 3.3 shows that K is inversely proportional to the water vapor mass transfer resistance, previously defined by Eq. 3.1.

From the above relationship, it is possible to estimate the experimental values of K from experimental values of the primary drying rate, denoted by $\dot{m}$, over the sublimation period corresponding to the freeze-dried layer thickness, L_{dry}, by the following relationship:

$$K_{exp} = \frac{L_{dry}}{P_s - P_c}\frac{\tilde{R}T_s}{\tilde{M}_w} \cdot \dot{m} \tag{3.4}$$

Nakagawa *et al.* (2007a) interpreted the dependence of the water vapor mass transfer permeability of the dried layer on ice crystal morphologies by using this relationship for different nucleation temperatures. The increase in the nucleation temperature was expected to increase the water vapor mass transfer permeability of freeze-dried materials and to contribute to acceleration of the primary sublimation rates during freeze-drying.

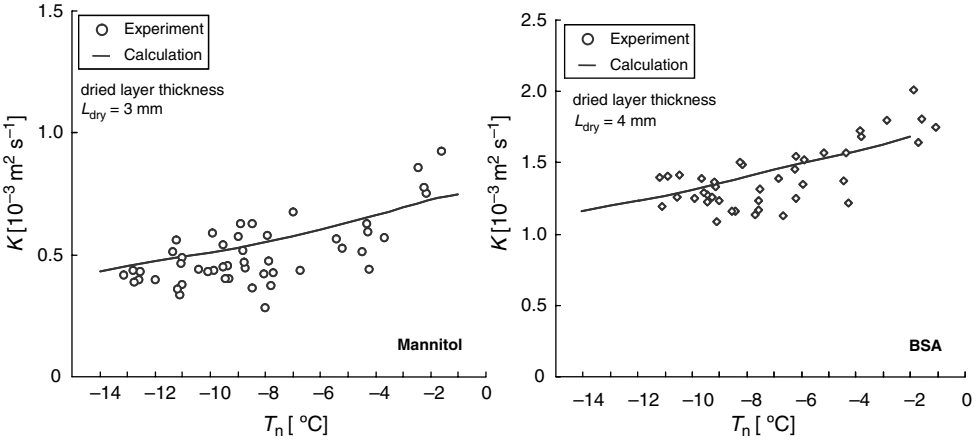

Fig. 3.20 Comparison of experimental and estimated dried layer permeability values according to Nakagawa *et al.* (2007a).

The experimental values of permeability, K_{exp}, plotted in Fig. 3.20 correspond to mean values of dried layer thickness, L_{dry}, of about 3 and 4 mm for the mannitol and the BSA systems, respectively.

On the other hand, the dried cake permeability values were theoretically estimated by the same authors from values of the mean size of the ice crystals by assuming that the freeze-dried cake texture could be represented by a bundle of capillary tubes (mean diameter, denoted $\bar{d}_{pore}$). Under conditions of molecular flow in the Knudsen regime (Kn = 4) this theoretical freeze-dried layer permeability, denoted by K_{model}, was estimated by the following equations:

$$K_{model} = \frac{\varepsilon}{\tau} D_k \Omega \tag{3.5}$$

where the water vapor Knudsen diffusivity, D_k, was expressed by the following relationship:

$$D_k = \frac{1}{3}\sqrt{\frac{8\tilde{R}T_s}{\pi\tilde{M}_w}} \cdot \bar{d}_{pore} \tag{3.6}$$

Here, Ω represents a total flow contribution factor, equal to:

$$\Omega = \frac{1}{1 + \bar{d}_{pore}/\lambda} \tag{3.7}$$

where λ represents the mean free path of the gas molecules under selected sublimation conditions.

For this estimation, Nakagawa *et al.* (2007a) assumed that the mean ice crystal size corresponded to the pore diameter, $\bar{d}_{pore}$ in Eqs. 3.6 and 3.7. The form factor ε/τ, in Eq. 3.5, has been considered as an empirical constant and was identified from a set of experimental data. The experimental and calculated values, denoted by K_{exp} and

K_{model}, respectively, plotted in Fig. 3.20, show pretty good agreement. These data clearly show that the water vapor mass transfer resistance decreases as the nucleation temperature increases, so that the drying process can be accelerated by increasing the nucleation temperature. This tendency is in logical agreement with the ice crystal size estimation obtained both from image analysis and from the model prediction.

Consequently, it is confirmed that, for a given system, the mass transfer phenomena during the sublimation step of the freeze-drying process are significantly dependent on the morphology of the ice crystals and, in consequence, significantly dependent on the nucleation temperatures of the supercooled formulation.

3.3.5
Importance of Temperature Control

Freeze-drying is a mild drying process during which the temperature profile of the sample all through the freezing step and the two subsequent drying steps has great importance, not only for the operating costs of the whole process – costs that are generally pretty high due to very low total gas pressure and the temperatures involved for fragile and thermosensible drugs – but also for the many quality attributes required by the stringent quality standards of such products.

As the sample is cooled, supercooling (about 10–15 K) below the equilibrium freezing point takes place before nucleation and crystal growth can occur, accompanied by a rise in the temperature of the solution up to the equilibrium freezing point (cf. Fig. 3.3). Then, the sample product temperature decreases slowly until freezing of most of the free water is completed and, then, it decreases rapidly down to the shelf temperature. The ice crystal growth induces an increase in viscosity and concentration of the cryo-concentrated solution. Other solutes of the formulation, such as sodium chloride, buffer salt components or other low molecular inorganic excipients, may also crystallize. Generally the drug (API) itself, the organic components and the high molecular excipients do not crystallize; they stay amorphous and diluted in a glassy phase containing some amount of unfrozen water. A large part of this unfrozen water is separated during the last process step by means of diffusion inside the amorphous phase and/or by desorption from the pore surfaces of the freeze-dried matrix. As previously indicated, primary and secondary drying steps are conducted at very low total gas pressure (5–60 Pa) and at low sublimation front temperatures (−10 to −40 °C) during the sublimation step, whereas the product temperature is increased above the ambient temperature during the secondary drying step (usually to levels between 20 and 40 °C in the case of thermosensible drugs). The main objective of these two drying steps is to generate a form of the labile drug that is stable for many months. The drug is normally a parenteral product that has to be rehydrated before injection. The therapeutic or biological activity of the final product (vaccines, for example) is quite sensitive to the product temperature history from the first step (freezing) up to the last step (desorption) when the temperature is strongly increased. The rate of sublimation increases rapidly with the sublimation front (or product) temperature by about a factor of two for temperature increases of

6 K. Process efficiency (primary and secondary drying times) is directly related to these main operating parameters. It must be borne in mind that too high processing temperatures will compromise several important quality factors (therapeutic or biological activity, mechanical structure resistance, porosity, appearance, crack formation, etc.).

Many experimental studies have shown that, for systems which contain one solute that gives a crystalline phase in solid state, the primary drying step must be conducted below the eutectic temperature. Nevertheless, most drug formulations do not crystallize or have high eutectic temperatures so that the eutectic temperature limit is not very often an issue in freeze-drying cycle optimization, if we except the systems containing high concentrations of NaCl, this salt having a eutectic temperature around −20 °C. Otherwise, with amorphous or glassy systems, the sublimation step must be carried out below the vitreous transition temperature or below the collapse temperature, which is generally a few degrees above the vitreous transition temperature of the system. If the product is sublimed above this limiting vitreous transition temperature, the solid phase collapses, because it has enough fluidity to induce a viscous flow when the ice is removed from the frozen sample. This collapse will lead to a loss of mechanical resistance of the dried cake structure and will result in higher moisture content and in a loss of biological activity with some protein formulations (vaccines). Some other defects like an increase in the rehydration times or some loss of pharmaceutical performance and elegance of the cake can also occur.

3.3.6
Influence of Operating Conditions on Sublimation Kinetics

For many materials (gels, ceramics, wood, etc.), it is well known that the drying kinetics curves are very helpful for understanding the influence of the main operating parameters (temperature, total gas pressure) on many quality factors like color changes, dried material shrinkage, risk of crack formation, crust formation (solute crystallization, for example in liquid containing sugars), the formation of a vapor-tight skin of polymers (for example during the reactive drying of paintings), and so on. Thus, examination of the drying curves associated with the temperature profiles inside the product constitute an important tool and a pertinent guide for setting up and optimizing the drying conditions of many types of manufactured products, including pharmaceuticals or drugs during lyophilization cycles.

Moreover, the use of drying curves enables detection of the main governing mechanisms that control the heat and mass transfer phenomena and, in this way, enables one to determine the main input physical variables for setting up and validating software for the control and monitoring of the freeze-dryer (shelf temperature or total gas pressure).

The influence of shelf temperature and of sublimation chamber total gas pressure on the drying curve ($\bar{X}$(t)) and on the drying rate curve ($-\frac{d\bar{X}(t)}{dt}$) is discussed below. As observed by many authors during the drying of different types of materials, for example during the convective or infrared reactive drying of thin coating films, the

classical drying curves (moisture content, drying rates, mean product temperature) as a function of time exhibit roughly three drying periods:

- An acceleration period during which the sublimation rate increases continuously (transient sublimation state).
- A quasi-stationary period during which the sublimation rate is quite constant. This corresponds to a quasi-steady state with an approximately constant sublimation front temperature. The duration of this plateau period seems to decrease as the sublimation temperature increases. The experimental data presented in Fig. 3.21 show that the sublimation rate increases by about a factor of two for an increase of 20 °C in the shelf temperature (from −25 to −5 °C).
- A decreasing drying rate period where the drying rates decrease rapidly with a simultaneous monotonic and significant increase in the mean product temperature.

Furthermore, it is quite surprising to observe that the scientific literature on freeze-drying in vial configuration contains little data concerning such drying curves. Nevertheless, some data are available (Genin *et al.*, 1996) and show that a shelf temperature increase from 0 to 25 °C increases the drying rate by a factor of two; the same drying rate increase (factor of two) was obtained by increasing the total gas pressure by a factor of 100. Additionally, some experimental studies have been carried out by using a microbalance placed inside the freeze-drying chamber (Roth *et al.*, 2001; Jun *et al.*, 2004). The sublimation data reported by these authors show three desiccation periods. These data also indicate the importance of vial package density which affects the values of the sublimation rate.

A coherent set of drying kinetics data concerning the freeze-drying of model pharmaceutical formulations in vials under standard operating conditions, namely at very low total gas pressure (10–26 Pa) and at low sublimation temperature (−5 to −25 °C) was published recently by Hottot *et al.* (2007). A typical set of sublimation rate data gained by these authors is presented in Fig. 3.21 concerning the influence of

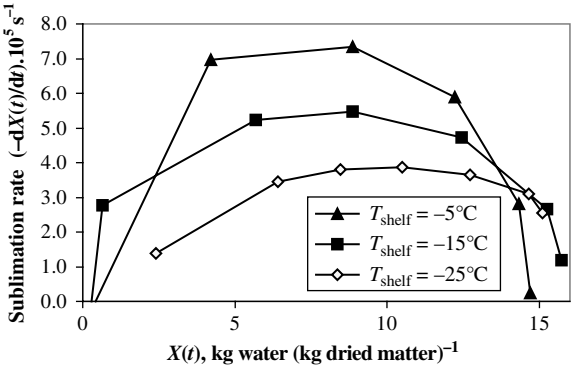

Fig. 3.21 Sublimation rates for different shelf temperatures at $P = 18$ Pa according to Hottot *et al.* (2007).

the shelf temperature. These data show that, for a constant total gas pressure ($P = 18$ Pa), a plateau appears at mean water content values located in the range $5\,\mathrm{kg\,kg^{-1}} < X(t) < 13\,\mathrm{kg\,kg^{-1}}$. Moreover, the sublimation rates corresponding to the height of this plateau increase with the shelf temperature, which means that they also increase with the sublimation front temperature. Further experimental results by the same authors for the two other pressures investigated (10 and 26 Pa) show similar trends. For the standard sublimation conditions of Hottot *et al.* (2007), the domain of water content with an approximately constant drying rate seems to correspond to a stationary state of sublimation, as generally assumed in simple front models. Such a model has been implemented by the same authors for the purpose of validation by comparing with measured sublimation kinetics (Hottot *et al.*, 2006b). In total, these experimental data show that, under standard freeze-drying conditions for very thermosensible drugs, the sublimation kinetics are mainly dependent on the sublimation front temperature which is fixed by the shelf temperature. Therefore, shelf temperature is the key input parameter for the control of important textural (or physical) quality features and of therapeutic activity factors.

The set of data plotted in Fig. 3.22 shows only a slight influence of the chamber total gas pressure on the sublimation kinetics. These observations are in agreement with the results reported by Kuu *et al.* (2005) who proposed an interesting approach to transferring laboratory scale freeze-drying data to industrial scale conditions. The same authors observed that the chamber total pressure only has a significant influence on the drying kinetics when the shelf temperature is maintained below $-15\,^{\circ}$C, see also Trappler (2001); Rambhatla and Pikal (2003). Consequently, we conclude that the sublimation process under standard conditions of very low temperature and total gas pressure, as encountered in thermosensible drugs freeze-drying, is mainly governed by the overall heat transfer flux to the sublimation

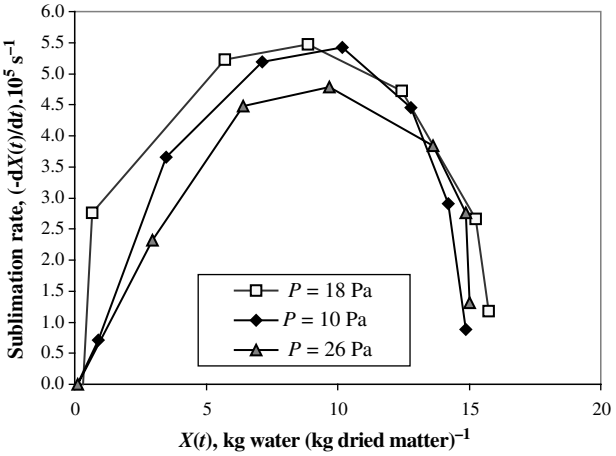

Fig. 3.22 Sublimation rates for different total gas pressures at $T_{shelf} = -15\,^{\circ}$C, according to Hottot *et al.* (2007).

front, namely by the heat conduction flux from the plate through the vial bottom and also by the radiation flux coming from the vial surroundings, specifically from the sidewalls of the sublimation chamber and from the upper shelf.

The previously discussed experimental data have recently been extended to pharmaceutical formulations with organic co-solvent – active principle ingredient (API) + water + *tert*-butyl alcohol (TBA) – by Daoussi *et al.* (2009) who used an automatic microbalance placed inside the product chamber to determine the sublimation kinetics. The same shapes of sublimation kinetics curves were observed.

The strong influence of the shelf temperature, regardless of the total gas pressure, proves that the sublimation process under conditions of very low total gas pressure and temperature is still mainly controlled by heat transfer, as in the case of aqueous formulations (Fig. 3.23). The sublimation rate was not a monotically increasing function of total gas pressure but reached a maximal value at the intermediate total gas pressure investigated (15 Pa) then decreased. Daoussi *et al.* (2009) observed that the use of organic co-solvent reduced considerably the sublimation times to around 3 h, these values being 10 to 11 times lower than the values observed with pure aqueous formulations under the same operating conditions of temperature and pressure. Simultaneously, the organic co-solvent allowed preservation of the main quality factors of the freeze-dried product (residual solvent and water contents, visual appearance, color, cake permeability, rehydration times, stability, etc.). This proves that formulations with organic co-solvent lead to sublimation times comparable with drying times observed with agitated vacuum contact dryers; consequently, these organic formulations, if suitable for stabilizing the investigated active principle (API), can significantly reduce the operating costs of freeze-drying compared with those for pure aqueous systems.

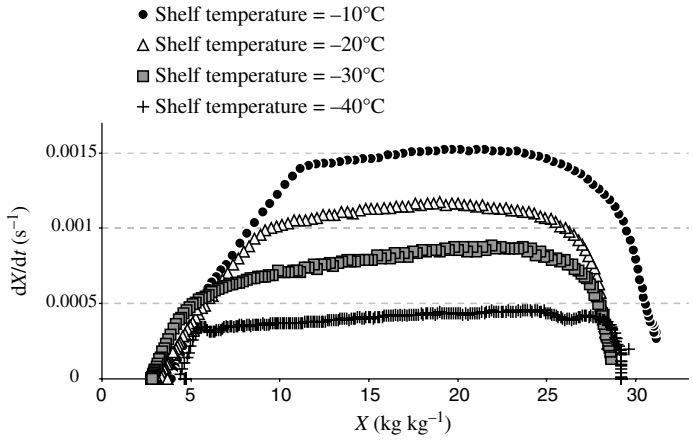

Fig. 3.23 Drying kinetics as a function of total solvent (water + TBA) content at different shelf temperatures; formulation at 20% water + 80% TBA (by mass). Influence of shelf temperature. According to Daoussi *et al.*, 2009.

3.4
Product Quality and Stability During Drying and Storage

3.4.1
Product Quality and Formulation

The final product quality attributes are strongly related to the level of optimization of the composition of the liquid formulation, which is a multidisciplinary and challenging problem usually solved by tedious experimental approaches in the development of freeze-drying cycles. The topics of formulation that involve complex knowledge of physical chemistry, biochemistry and biology are outside the scope of this chapter. However, general concepts that are generally applied are summarized hereafter.

The mechanisms that govern product stability during storage are the same as those involved during the drying steps, the only difference being the water content and the time scales for the two phenomena. For example, in the case of pharmaceutical proteins, the role of the stabilizer is to slow down the degradation reactions by introducing high activation energy barriers which prevent the formation of significant amounts of denatured protein forms. Two main concepts are generally proposed to explain the role of excipients in promoting stabilization effects during the two drying steps and during the storage step: the vitrification hypothesis and the water substitution hypothesis (Pikal, 1999a).

The "vitrification" concept relies on the experimental observation that efficient stabilizers are always convenient glass-former materials with very high viscosity at temperatures below the glass transition temperature. Several experimental studies have pointed out a sharp decrease in mobility (chain fluctuation and chain rotation) and a consequent decrease in reactivity when the glass transition temperature is approached.

The "water substitute" concept states that the stabilizer replaces the water and forms hydrogen bonds with the protein, like water also does. These bonds maintain the native protein conformation and, in this way, stabilize the protein. The water substitution hypothesis has been confirmed either by spectroscopy studies (FTIR), or by experimental observations that have shown that the most efficient stabilizers are sugars which form strong hydrogen bonds with the protein. Indeed, freeze-dried systems with loss of activity present notably altered IR spectra.

Nevertheless, some exceptions exist and not all additives which are good stabilizers show chemical and bonding properties similar to water. Many experimental data have shown that the stabilization of fragile and thermosensible pharmaceutical proteins requires a lyoprotectant that is a good glass-former, leading to a single amorphous solid phase, with a moderate interaction with the protein surface to avoid phase separation (crystallization, etc.).

As already indicated, nucleation temperature, nucleation rates and solvent crystal growth rates are of crucial importance for the morphology and for the structure of the resulting freeze-dried product. Freeze-drying generally leads to an

amorphous phase (e.g., with sugars) that often crystallizes during the secondary drying period (Pikal, 1999b). Moreover, lyophilization can also produce metastable crystalline forms directly from aqueous solutions upon freezing, with formation of an amorphous solid during secondary drying. This crystallization behavior depends on multiple factors, such as the freezing rate, the nature and concentration of the solutes and the nature and concentration of the additives (cryoprotectants, lyoprotectants, etc.).

3.4.2 Product Quality and Polymorphism

The formation of polymorphs and various hydrates can also affect many quality factors and must be carefully considered in stability criteria (Pikal, 1999b; Morris *et al.*, 2001). Many experimental results have shown that crystallization from aqueous solutions is favored by higher concentrations of crystallizable solute. On the contrary, the presence of high concentrations of other solutes that remain amorphous generally prevents the crystallization of the main possible crystallizable solute. For example, the crystallization of mannitol, which is easy if this solute is quite pure, becomes improbable in the presence of other solutes in high concentration.

Polymorphism, which is a frequent and well-known phenomenon in drug crystallization, has a direct influence on the physical and chemical properties of the freeze-dried cake and, consequently, can impact drastically the manufacturing aptitude and the performances of dosage forms (tablets or capsules). Polymorphism has a direct influence on the dissolution kinetics variations and, thus, it also influences the bioavailability and the stability of the API. Due to the complexity of phase changes during freeze-drying – they are related to formulation, process and storage conditions – these problems are often ignored in the pharmaceutical R&D and industry. This may have important consequences because the process is usually long and expensive and, thus, undesired phase changes can greatly modify the processing times and the final therapeutic or biological activity of the freeze-dried products (for example, with pharmaceutical proteins). In some cases, drug crystallization significantly increases its stability. Conversely, the crystallization of one excipient – especially the crystallization of a buffer or a stabilizer in protein formulations – leads generally to a significant loss of stability (Pikal, 1999b). On the other hand, crystallization of poorly soluble drugs may increase the reconstitution times or even lead to incomplete dissolution, due to the better solubility of the amorphous phases in comparison to the respective crystalline forms.

Crystallization during the storage step is also sensitive to the residual water content and to the storage temperature. Generally, recrystallization is more probable at storage temperatures higher than the vitreous transition temperature, but with some systems, and for long storage times, recrystallization can also occur at temperatures below the glass transition temperature.

Crystallization can also exert a major impact on the freeze-drying cycle duration, since it modifies the composition of the solute phase and, thereby the value of T_g'. This influence can be positive or negative, depending on when crystallization occurs and on what component crystallizes: an increase in T_g', as would be produced by crystallization of inorganic salts, would allow sublimation at higher temperatures and thus result in shorter sublimation times with a positive effect on operating costs. On the contrary, a decrease in T_g' would require that the sublimation step be run at lower temperatures, leading to longer sublimation times (negative impact). It is well known that mannitol, which is a commonly used excipient as a bulking agent, can lead to vial breakage problems if its crystallization occurs during the primary drying step, so that the crystallization of mannitol from API formulations has to take place during the freezing step to avoid this problem (Pikal, 1999b, 2002).

3.5 Conclusions

The strong coupling between final quality parameters and transport phenomena poses serious challenges for the optimization of the drying cycles used in modern industry for manufacturing many products and materials, particularly in the pharmaceutical industry. The understanding of these relationships is still more crucial in the case of freeze-drying processes of fragile and very thermosensible materials, such as pharmaceuticals and drugs. Complex and interdependent phenomena of phase transition (ice nucleation, vitreous transition of cryoconcentrated phase, polymorphism) occur during freeze-drying, inducing sharp changes in the morphological and rheological properties of the material. The stresses generated during the freezing and the drying steps modify the native conformational structure of thermosensible active principles like pharmaceutical proteins and, in this way, they also modify their therapeutic activity. Removal of water by two-phase changes (crystallization, sublimation) induces more or less shrinkage, which changes the volume fraction of the phases and thus modifies the values of the main parameters of heat and mass transport that takes place under severe conditions (low temperature and high vacuum). Transport parameters are not generally available in the literature.

Furthermore, the final therapeutic activity and stability of the drug during the storage period are strongly dependent on the residual moisture content, on eventual moisture gradients and on the temperature history of the product during the whole freeze-drying process. These problems can be generally solved by tedious experimental approaches.

As explained in this chapter, the freezing and drying requirements for the control of the main quality factors are strongly coupled and related to the system formulation, namely to the state diagram data, which represent the key data in setting up the lyophilization cycles at the pilot and then industrial scales. As a consequence, fine and advanced physical modeling of these freezing and drying steps, with enhanced

computer facilities, can, in the future, play an important role and lead to a more scientific and more rational methodology for the control of these physical quality factors involved in the optimization of freeze-drying processes of fragile pharmaceuticals.

Consequently, a common effort should be made to establish and complete the data basis concerning the numerous thermodynamic, thermophysical, transport and rheological properties necessary for modeling and simulating the different steps of this complex mild drying process. Moreover, the methods available for the characterization of most of these end-use properties should be improved and additional characterization methods should be adapted from other research fields (material science, applied biochemistry, physical chemistry, etc.). Improved characterization methods promise a better description and a safer control of numerous end-use properties for existing freeze-dryers as well as for new machines with more possibilities to better comply with more and more severe quality requirements in the future. The use of non-invasive sensors or of rapid non-intrusive methods for on-line and *in situ* estimation of the main parameters of the process could also help to overcome the difficulties observed, for example, the artifacts resulting from invasive sensors inserted inside vials and presently commonly used.

Additional Notation Used in Chapter 3

h	solution height inside the vial	m
K_v	overall heat transfer coefficient	$W\,m^{-2}\,K^{-1}$
K	dried layer permeability	$m^2\,s^{-1}$
R_p	water (solvent) vapor mass transfer resistance	$Pa\,m^2\,s\,kg^{-1}$
T'_g	glass transition temperature at maximum concentration of the cryo-concentrated phase	K, °C
T_g	glass transition temperature temperature	K, °C
T_n	nucleation temperature	K, °C
T_s	sublimation front temperature	K

Greek letters

λ	mean free path of gas molecules	m
τ	tortuosity factor	
Ω	total flow contribution factor	

Subscripts

c	chamber
i	interface
s	sublimation
p	product

Abbreviations

API	active principle ingredient
BSA	bovine serum albumin
DSC	differential scanning microscopy
FTIR	Fourier transform infra-red
IR	infra-red
MDSC	modulated scanning microscopy
MTM	manometric temperature measurement
NMR	nuclear magnetic resonance
PAR	pressure rise analysis
US	ultrasound
SEM	scanning electron microscopy

References

Bardat, A., Biguet, J., Chatenet, E., Courteille, F., 1993. Moisture measurement: A new method for monitoring freeze-drying cycles. *J. Parenteral Sci. Tech.* **47**(6): 293–299.

Berger, K. G., White, G. W., 1971. An electron microscopical investigation of fat destabilisation in ice cream. *J. Food Technol.* **6**: 285–294.

Caillet, A., Cogne, C., Andrieu, J., Laurent, P., Rivoire, A., 2003. Characterization of the structure of ice cream by optical microscopy: Influence of freezing parameter on ice crystal structure. *Lebensm. -Wiss. u. -Technol.* **36**: 743–749.

Chouvenc, P., Vessot, S., Andrieu, J., Vacus, P., 2004a. Optimization of the freeze-drying cycle: A new model for pressure rise analysis. *Drying Technol.* **22**(7): 1577–1601.

Chouvenc, P., Vessot, S., Andrieu, J., Vacus, P., 2004b. Optimization of the freeze-drying cycle: Characterization of annealing effects by the pressure rise analysis method. *Proceedings of 14th International Drying Symposium (IDS 2004)*, Sao Paulo, Vol. A, 359–365.

Chouvenc, P., Vessot, S., Andrieu, J., 2006. Experimental study of the impact of annealing on ice structure and mass transfer parameters during freeze-drying of a pharmaceutical formulation. *PDA J. Pharm. Sci. Tech.* **60**(2): 95–103.

Chow, R., Blindt, R., Chivers, R., Povey, M., 2003. The sonocrystallization of ice in sucrose solutions: Primary and secondary nucleation. *Ultrasonics* **41** (8): 595–604.

Chow, R., Blindt, R., Chivers, R., Povey, M., 2005. A study on the primary and secondary nucleation of ice by power ultrasound. *Ultrasonics* **43**(4): 227–230.

Daoussi, R., Vessot, S., Andrieu, J., Monnier, O., 2009. Sublimation kinetics and sublimation end-points during freeze-drying of pharmaceutical active principle with organic co-solvent formulations. *Chem. Eng. Res. Des.*, **87**: 899–907.

Faydi, E., Andrieu, J., Laurent, P., 2001. Experimental study and modelling of the ice crystal morphology of model standard ice cream, Part I: Direct characterization method and experimental data. *J. Food Eng.* **48**: 283–291.

Franks, F., 1990. Freeze-drying: from empiricism to predictability. *Cryo-Lett* **11**: 93–110.

Genin, N., Rene, F., Corrieu, G., 1996. A method for on line determination of residual water content and sublimation end point during freeze drying. *Chem. Eng. Process.* **35**: 255–263.

Hickling, R., 1965. Nucleation of freezing by cavity collapse and its relation to cavitation damage. *Nature* **206**: 915–917.

Hottot, A., Vessot, S., Andrieu, J., 2004. A direct characterization method of the ice morphology: Relationship between mean crystals size and primary drying times of freeze-drying processes. *Drying Technol.* **22**: 2009–2021.

Hottot, A., Vessot, S., Andrieu, J., 2005. Determination of mass and heat transfer parameters during freeze-drying cycle of pharmaceutical products. *PDA J. Pharm. Sci. Tech.* **59**: 138–153.

Hottot, A., Vessot, S., Andrieu, J., 2006a. Freeze-drying of pharmaceuticals in vials: Influence of freezing protocol and sample configuration on ice morphology and freeze-dried cake texture. *Chem. Eng. Process.* **46**: 666–674.

Hottot, A., Peczalski, R., Vessot, S., Andrieu, J., 2006b. Freeze-drying of pharmaceutical proteins in vials: Modeling of freezing and sublimation steps. *Drying Technol.* **24**: 561–570.

Hottot, A., Andrieu, J., Vessot, S., 2007. Sublimation kinetics during freeze-drying of pharmaceutical protein formulation. *Drying Technol.* **25**: 1–6.

Hottot, A., Nakagawa, K., Andrieu, J., 2008. Effect of ultrasound-controlled nucleation on structural and morphological properties of freeze-dried manitol solution. *Chem. Eng. Res. Des.* **86**: 193–200.

Hottot, A., Andrieu, J., Vessot, S., Shalaev, E., Gatlin, L. A., Ricketts, S., 2009a. Experimental study and modelling of freeze-drying in syringe configuration, Part I: Freezing step. *Drying Technol.* **27**(1): 40–48.

Hottot, A., Andrieu, J., Hoang, V., Shalaev, E. Y., Gatlin, L. A., Rickett, S., 2009b. Experimental study and modelling of freeze-drying in syringe configuration, Part II: Mass and heat transfer parameters and sublimation end-points. *Drying Technol.* **27**(1): 49–58.

Inada, T., Zhang, X., Yabe, A., Kozawa, Y., 2001. Active control of phase change from supercooled water to ice by ultrasonic vibration 4, Part 1: I Control of freezing temperature. *Int. J. Heat Mass Transfer* **44**: 4523–4531.

Jun, X., Jeffery, H., Volker, L., Wang, D. Q., 2004. Investigation of freeze-drying sublimation rates using a freeze-drying microbalance technique. *Int. J. Pharm.* **279** (1–2): 95–105.

Kochs, M., Korber, I., Heschel, B., Nunner, B., 1993. The influence of the freezing process on vapour transport during sublimation in vacuum freeze-drying of macroscopic samples. *Int. J. Heat Mass Transfer* **34**: 1727–1738.

Kuu, W. Y., Hardwick, L. S., Akers, M. J., 2005. Correlation of laboratory and production freeze drying cycles. *Int. J. Pharm.* **302**: 56–67.

Mahdjoub, R., Chouvenc, P., Seurin, M. J.L.,, Andrieu, J., Briguet, A., 2006. Sucrose solution freezing studied by magnetic resonance imaging. *Carbohydr. Res.* **341**: 492–498.

Mckenzie, A. P., 1975. Collapse during freeze-drying: Qualitative and quantitative aspects, in *Freeze-drying and Advanced Food Technology* (eds S. A. Golblith, L. Rey, W. W. Rothmayer). Academic Press, London, pp. 277–307.

Milton, N., Pikal, M. J., Roy, M. L., Nail, S. L., 1997. Evaluation of manometric temperature measurement as a method of monitoring product temperature during lyophilization. *PDA J. Pharm. Sci. Tech.* **51**(1): 7–16.

Morris, K. R., Griesser, U. J., Eckhardt, C. J., Stepwell, J. G., 2001. Theorical approaches to physical transformations of active pharmaceutical ingredientds during manufacturing processes. *Adv. Drug Deliv. Rev.* **48**: 91–114.

Morris, J., Morris, G. J., Taylor, R., Zhai, S., Slater, N. K. H., 2004. The effect of controlled nucleation on ice structure, drying rate, and protein recovery in vials in a modified freeze-dryer. *Cryobiology* **49**: 308–309.

Nakagawa, K., Hottot, A., Vessot, S., Andrieu, J., 2006. Influence of controlled nucleation by ultrasounds on ice morphology of frozen formulations for pharmaceutical proteins freeze-drying. *Chem. Eng. Process.* **45**: 783–791.

Nakagawa, K., Hottot, A., Vessot, S., Andrieu, J., 2007a. Modeling of freezing step during freeze-drying of drugs in vials. *AIChE J.* **53**(5): 1362–1372.

Nakagawa, K., Murakami, W., Andrieu, J., 2007b. Influence of freezing conditions on

crystalline structure of mannitol. *Proceedings of 16th International Drying Symposium (IDS 2008)*, Hyderabad, India, Vol. C, 1794–1800.

Obert, J. P., 2001. *Modélisation, optimisation et suivi en ligne du procédé de lyophilisation: Application à l'amélioration de la productivité et de la qualité des bactéries lactiques lyophilisées*. Diss. INRA Université Paris-Grignon, France.

Patapoff, T., Overcashier, D. E., Hsu, C. C., 1999. Lyophilization of proteins formulations in vials: Investigation of the relationship between resistance to water vapour flow during primary drying and small-scale product collapse. *J. Pharm. Sci.* **88**(7): 688–695.

Patapoff, T., Overcashier, D. E., 2002. The importance of freezing on lyophilization cycle development. *Biopharm.* **3**: 16–22.

Petersen, A., Rau, G., Glasmacher, B., 2006. Reduction of primary freeze-drying time by electric field induced ice nucleus formation. *Heat Mass Transfer* **42**: 929–938.

Pikal, M. J., Roy, M. L., Shah, S., 1984. Mass and heat transfer in vial freeze drying of pharmaceuticals: Role of the vial. *J. Pharm. Sci.* **73**(9): 1224–1237.

Pikal, M. J., 1985. Use of laboratory data in freeze-drying process design: Heat and mass transfer coefficients and the computer simulation of freeze drying. *J. Parenteral Sci. Tech.* **39**(3): 115–139.

Pikal, M. J., 1990. Freeze-drying of proteins, Part I: Process design. *Biopharm.* **3**: 18–27.

Pikal, M. J., 1992. Freeze-drying, in *Encyclopedia of pharmaceutical technology.* Vol. 6, (eds. J. Swarbrick and J.C. Boylan), Marcel Dekker, New York, pp. 275–303.

Pikal, M. J., 1999a. Mechanisms of protein stabilization during freeze-drying and storage: The relative importance of thermodynamic stabilization and glassy state relaxation dynamics. *Drugs and Pharmaceutical Science*, **96**: 161–198.

Pikal, M. J., 1999b. Impact of polymorphism on the quality of lyophilised products, in *Polymorphism in Pharmaceutical solids* (ed. H. G. Brittazin). Marcel Dekker, New York, pp. 395–419.

Pikal, M. J., 2002. Lyophilization, in *Encyclopedia of Pharmaceutical Technology.* (eds. J. Swarbrick and J.C. Boylan),Marcel Dekker, New York, pp. 1299–1326.

Rambhatla, S., Pikal, M. J., 2003. Heat and mass transfer scale up issues during freeze drying, I: A typical radiation and the edge vial effect. *AAPS Pharm. Sci. Tech.* **4–2**(14): 1–10.

Rambhatla, S., Ramot, R., Bhugra, C., Pikal, M. J., 2004. Heat and mass transfer scale-up issues during freeze-drying, II: Control and characterization of degree of supercooling. *AAPS Pharm. Sci. Tech.* **5**(4): 1–8.

Roth, C., Winter, G., Lee, G., 2001. Continuous measurement of drying rate of crystalline and amorphous systems during freeze-drying using an in situ microbalance technique. *J. Pharm. Sci.* **90** (9): 1345–1355.

Roy, M. L., Pikal, M. J., 1989. Process control in freeze-drying: Determination of the end point of sublimation drying by an electronic moisture sensor. *J. Parenteral Sci. Tech.* **43** (2): 60–66.

Saclier, M., Peczalski, R., Andrieu, J., 2008. Modélisation de la nucleation de cristaux de glace déclenchée par ultrasons. *Récents Progrès en Génie des Procédés, Ed. SFGP 97, (8 pages)*.

Schneid, S., Gieseler, H., 2008. Evaluation of a new wireless temperature remote interrogation system (TEMPRIS) to measure temperature during freeze-drying. *AAP Pharm. Sci. Tech.* **9** (3): 729–739.

Searles, J. A., Carpenter, J. F., Randolph, T., 2001a. The ice nucleation temperature determines the primary drying rate of lyophilization for samples frozen on a temperature-controlled shelf. *J. Pharm. Sci.* **90**(7): 860–869.

Searles, J. A., Carpenter, J. F., Randolph, T., 2001b. Annealing to optimize the primary drying rate, reduce freeze-induced drying rate heterogeneity, and determine T'_g in pharmaceutical lyophilization. *J. Pharm. Sci.* **90**(7): 872–887.

Trappler, E., 2001. Scale-up strategy for a lyophilization process. *Am. Pharm. Rev.* **4** (3): 55–60.

Woinet, B., Andrieu, J., Laurent, M., Min, S. G., 1998. Experimental and theoretical study of model food freezing, Part II: Characterization and modelling of the ice crystal size. *J. Food Eng.* **35**(4): 395–407.

Zhai, Z., Taylor, R., Sanhes, R., Slater, N. K. H., 2003. Measurement of lyophilisation primart drying rates by freeze-drying microscopy. *Chem. Eng. Sci.* **58**: 2313–2323.

Zhang, X., Inada, T., Yabe, A., Lu, S. Kozawa, Y., 2001. Active control of phase change from supercooled water to ice by ultrasonic vibration, II: Generation of ice slurries and effect of bubble nuclei. *Int. J. Heat Mass Transfer* **44**: 4533–4539.

Zhang, X., Inada, T., Tezuka, A., 2003. Ultrasonic-induced nucleation of ice in water containing air bubbles. *Ultrason. Sonochem.* **10**(2): 71–76.